Master's Thesis.

Thermal and Crosstalk Aware Router Design for Wavelength-Routed Optical Network-on-Chip

Abhinay Prasad Manandhar

JUNE 2020

Under the supervision of

Dr. Ing. TSENG, TSUN-MING

Lehrstuhl für Entwurfsautomatisierung

Prof. Dr.-Ing. Ulf Schlichtmann

Technical University Munich, Germany.

Acknowledgement.

I would like to express my sincere gratitude to Technical University Munich, Germany for letting me fulfil my dream of being a student here. I would like to thank the ***"Lehrstuhl für Entwurfsautomatisierung"*** for giving me an opportunity to write an honour's thesis. I am grateful to **Dr. Ing. Tseng, Tsun-Ming** for your immense assistance and suggestion throughout the thesis work. I would like to thank **Prof. Dr.-Ing. Ulf Schlichtmann** for giving me permission to work under his department.

During the thesis work, I was able to acquire more knowledge in the field of Engineering, learning about new future technologies and advancements taking place in present state of art technologies.

Finally, I would like to thank my family and friends for constant support and strength.

Abstract

The current generation of IC chips is highly dense with multiple processing cores and different modules like RAM, controllers, and caches etc. The multicore system-on-chip (SOC) is a trending technology of the present generation enabling superfast computations, data processing, and signal processing leading to advancement in various fields of engineering. The multicore SOCs requires an interconnection of network with high bandwidth and superfast to cope up with the growing requirements of the consumer. These growing requirements can be fulfilled by a new generation of network-on-chip called Optical network-on-Chip. The optical network-on-chip has not been deployed in real world systems as it is prone to power losses and variations in temperature affects the performances of the SOCs. Optical network's performance depends on the efficiency of the optical routers. Simulation tools are used to simulate the behaviour of optical routers to evaluate the overall performances of the optical network-on-chip. In the past, although several optical routers has been proposed by various researchers, the quest of modelling an efficient optical router is still in a conundrum. The primary aim of the thesis is to design a 5x5 optical router for mesh-based network topology and analyze router characteristic with the help of two simulation software, Optical Crosstalk and Loss Analysis Platform (CLAP) and Optical Thermal Effect Modelling Platform (OTEMP). The simulations will provide observations regarding various losses and power consumption of the modelled routers. The simulation results of the modelled routers are compared with other existing optical routers in order to have clarity about the improvements in designed router's performance. This work also provides guidelines for modelling an optical router which can fulfil the growing requirements of modern day multicore SOC.

Chapters	Contents	Page no.
1	Introduction	4 - 6
2	Overview on Optical Router and Networks	7 - 17
	2.1 Related to Optical Routers.	11 - 14
	2.2 Different Network topologies of Optical Network-on-Chip	14 - 16
	2.3 Routing Algorithm	16 - 17
3	Challenges faced by Optical Network-on-Chip and Mathematical modelling	18 - 31
	3.1 Crosstalk Noise in Basic Photonics Devices	19 - 20
	3.2 Crosstalk Noise in Optical Interconnection Network.	20 - 21
	3.3 Analytical Modelling of Crosstalk Noise of Basic Optical Device	21 - 24
	3.4 Thermal Model of Optical Network-on-Chip	24 - 31
4	Introduction to Simulation tools	32 - 42
	4.1 CLAP – Crosstalk and Loss Analysis Platform	32 - 33
	4.2 OTEMP – Optical Thermal Effect Modelling Platform	34 - 35
	4.3 Router Modelling using CLAP Simulation Tool.	36 - 42
5	Case Study of Todays Optical Network-on-Chip	43 -48
	5.1 observation from Past Router Models	44 - 45
	5.2 Objectives Behind Modelling Optical Routers	45 - 46
	5.3 Modelled Routers	47 - 48
6	Comparison of Optical Routers	49 - 65
	6.1 Comparison Between Modelled Routers on Router Level	49 - 54
	6.2 Comparison Between CRUX and RC1.3 in Router Level	55
	6.3 Comparison Between Modelled Routers on Network Level	56 - 54
	6.4 Final Hypothesis	64 - 65
7	Thermal Behaviour of Modelled Routers with OTEMP tool	66 - 75
	7.1 OTEMP Simulations and Observation.	69 - 75
8	Conclusion	76
	References	

Chapter1.

Introduction

In the era of superfast computing, it is an utmost necessity that the computing system performs at an ultra-high speed for processing enormous amounts of data. Data processing consumes more energy, bandwidth and speed and hence the operating cores must have good synchronization in order to perform effectively and efficiently. The synchronization is achieved when the communicational network is fast and efficient. Until now the electronics network-on-chip has played a vital role in maintaining synchronization between various modules on-chip with different network architectures and routing topologies but as the demand for speed and bandwidth is growing progressively, the electronic network-on-chip is failing to provide the required performances due to the lack of scalability of electronic interconnects, available bandwidth and power consumption, mentioned in [20]. The performance degradations of electronic interconnect has encouraged the design engineers and researchers to come up with a new technology called "Optical Network-on-Chip-ONoCs". ONoCs are the interconnects of tomorrow, providing faster speeds and enormous amount of bandwidth which will enable processing big chunks of data in a short amount of time and with less energy dissipation compared to electronics network-on-chip. In the past, the fabrication of optical interconnect was not practically realizable due to shortcomings of fabrication processes. At present, advancements in fabrication processes have led to the manufacturing of optical elements which are required to practically realize the optical interconnect. These optical interconnects use light as the carrier of data from one point to another point and therefore it will provide faster speed and large bandwidth to an optical link allowing Wavelength Division Multiplexing (WDM) during the communication process.

Today's multicore based SOC architecture contains tons of processor cores and different modules which are connected by a network inside a single chip. These multicore systems need interconnects like ONoCs which enables huge numbers of cores and modules to communicate with high data rates and minimum losses during an information exchange. At present, there are network architectures where a combination of electrical and optical networks is used to get desired speed and bandwidth, this type of network architecture is called hybrid network-on-chip architecture, mentioned in [8][20], where the optical network is stacked above the electronic network and a separate control system decides when to switch data packets between optical network and electronic network. The advances in silicon photonics have led to realization of optical elements for optical networks. The fundamental component of an optical network are optical routers. Many optical router designs have been proposed by various researchers in this field, such as Cygnus, Crossbar, CRUX, Optimized Crossbar and ODOR etc, as mentioned in [1]. Every proposed router is unique in terms of size, communication pattern, signal power, losses etc. For example, Cygnus is a low-power non-blocking 5x5 optical router. It uses 16 microring resonators, six optical waveguides and two optical terminators to implement a 5x5 switching function.

From [1], for on-chip optical routers, microring resonators (MRs) have been widely used as a wavelength-selective optical switch to perform the switching function. The fabrication of MRs was based on silicon waveguide with cross-section 500nm x 200nm and the insertion loss was about 0.5*dB.* It was indicated that the DC power consumption of a 12 μm-diameter MR in the order of 20μW. Based on the switching function of MRs, several 5x5 optical routers has been proposed for mesh or torus-based optical network topologies. Waveguide crossings in ONoCs do not affect the bandwidth, but cause additional losses and higher power consumption during the packet transmission. Each waveguide crossing introduces about 0.12*dB* insertion loss to the passing optical signals. Although the loss per crossing is small, a large number of crossings in the optical transmission path might lead to significant power consumption. Router model must contain a minimum number of MRs and waveguide crossings while carrying out necessary switching functions and thereby consuming less power, thereby minimizing losses.

In this work, an overview of existing optical networks and routers are provided which helps the readers to get acquainted with the theory behind the optical components and devices. This section also familiarizes the readers with the mechanisms of signal switching with the help of MRs and also provides insights to the existing optical routers. The following section will provide knowledge related to analytical methods and processes used by the fellow researchers to generate mathematical equations for crosstalk noise, insertion loss and thermo-optic effect for optical networks and routers.

An introduction to two simulation tools will be provided. The first simulation and modelling tool, named CLAP, will be used to model optical router and simulate the modelled router for signal power, crosstalk noise and Signal to Noise Ratio (SNR), while the other tool called as OTEMP will be used to observe the thermal effect on a given network architecture.

The main objective of the work is to model 5x5 optical routers which performs better than the present optical routers based on signal power consumption, crosstalk noise and SNR. In order to achieve the main objective, optical routers were designed using CLAP tool and simulations were carried out on router level as well as on network level. After the simulation results were obtained the modelled routers were compared against 5x5 optical CRUX optical router. At router level, the modelled routers were compared for their cost of optical resources, e.g., the number of MRs, waveguide crossings, and optical terminators. At network level, the routers were placed in an 8x8 Mesh based network topology and the observations were made based on signal power, crosstalk noise and SNR. The secondary objective was to observe the thermal effects on an 8x8 mesh-based ONoCs with modelled optical routers using the OTEMP simulation tool and observe the changes in total power consumption, worst case and average case, with changes in temperature. In order to create gradual temperature changes across a chip a Gaussian temperature distribution was assumed and simulations were performed and observations were evaluated according to the simulation results.

ONoCs are a new emerging technology in the field of integrated systems and this technology is a novel technology which has not been deployed in real world systems. Several research works are published with respect to various sections of ONoCs and researchers are working extensively to bring this technology to work efficiently in future integrated systems. This thesis is organized into three sections, first, chapter 2 and 3 will provide a brief insight to the ONoCs, which will provide various information regarding the routing algorithms, network topologies, optical elements and existing optical routers. These chapters will provide information regarding the limitations of ONoCs and the effect of temperature changes on ONoCs and its mathematical modelling. Secondly, chapter 4 leads to the introduction to the CLAP and the OTEMP tools, these two tools were used to evaluate the performance of the modelled routers. Last section, chapter 5 onwards the readers will be taken through the modelling process and two modelled optical routers, *RC1.1* and *RC1.3*, will be introduced. Detailed evaluation of the modelled router has been provided, starting from router level to network level simulation. Readers are provided with tabular as well as graphical forms of the simulation results for better understanding and observation. The section also compares the performance of the modelled routers with the today's state of the art optical router like CRUX and according to these comparison a hypothesis has been made which elaborates the pros and cons of the modelled optical routers over the existing optical routers. A final hypothesis have been made where reasons for considering the modelled router as a better performing router are given. The hypothesis will point out the good points about the modelled router design which makes it perform better than the existing router and also point out the limitations of the router design. It also points out the area where improvements can be achieved in the future. The last section also deals with thermal effects on optical networks. In this section, modelled routers were simulated for changes in temperatures and results provided the fluctuations in power consumptions due to the changes in temperature. In this section, a hypothetical Gaussian distribution of temperature across the chip is assumed because the in a real scenario, the temperature changes quickly from chip's edges towards the centre. Therefore, simulation with this distribution will result in analysing networks performance due to temperature changes.

………………

Chapter 2.

Overview on Optical Router and Networks

An ONoCs consists of basic optical components assembled together to form a network. First element is a laser source provided with a modulator which could be placed internally or externally on-chip so as to transform an electric signal into an optical signal. Mostly, the source is integrated internally on-chip and if an external source is used then the light will be injected into the optical system to chip via optical couplers. The silicon is a material of choice to develop this kind of optical system-on-chip because it has been widely used in the industry of microelectronics. We can benefit from the maturity of manufacturing technology of CMOS integrated circuits for a massive production of low cost optical circuits. The hybridization of CMOS integrated circuit components is possible and can occur at various levels.

Optical communication and integration technologies are the most attractive solutions for current and projected limitations in inter and intra chip communication. The introduction of photonics to network-on-chip in Multi-processor System-on-Chip (MPSoC) can potentially enhance the on-chip communication performances thanks to their capacity, transparency, and fundamentally lower energy consumption. The opportunity to use silicon photonics has been made possible by recent advances in nano-scale silicon photonics and considerable improvements in photonics integration with the CMOS chip manufacturing. In particular, the rapid progresses in the past few years in laser source, nano scale modulators, silicon waveguide and CMOS compatible detector has enabled the introduction of highly integrated photonic platforms for generating, switching and receiving optical signal with considerable high power efficiency and bandwidth as well as low latency. Furthermore, some currently available technologies, such as WDM, can boost the bandwidth of ONoCs. MRs can be fabricated on SOI substrate which has been used for CMOS based high performance low leakage system-on-chips. MRs has a diameter in a range of 3-10 um [19]. An ONoCs consists of optical routers and optical links. Optical routers forms the backbone of an optical network as it routes the data packets from one source to different destinations. Optical routers contain optical ports, waveguides, MRs, waveguide crossings, optical modulators and optical terminators. Optical router suffers from losses such as insertion loss, coherent crosstalk, incoherent crosstalk and propagation loss, therefore, while designing an optical router these losses and crosstalk must be kept to minimum such that the SNR of the whole router is positive and up to an acceptable level for a reliable communication between the sources and destinations.

The main component of an optical router is a 1x2 switching elements which helps to switch the direction of the signal from one direction to another direction of an optical router as shown in figure 1. The 1x2 switching elements are of two types:

1. Crossing Switching Element (CSE).
2. Parallel Switching Element (PSE).

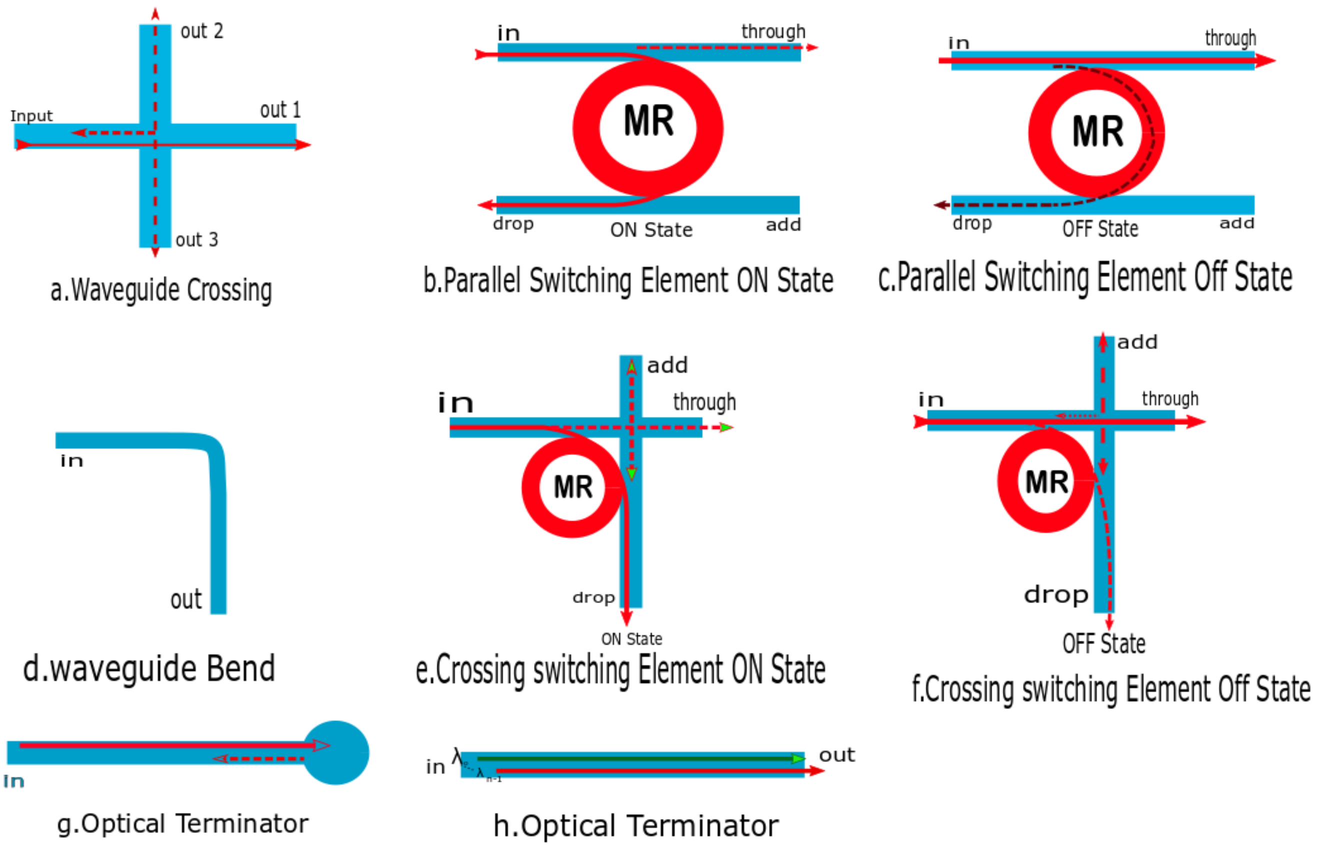

Figure 1: Optical elements of an optical Router

Both these 1x2 switching elements contains one MR and two optical waveguides. The 1x2 switching elements contains four ports - Input port, Drop port, Through port and Add port. MRs has different on-state and off-state resonant wavelength, λ_{on} and λ_{off} respectively. The MR of the switching element can be tuned to particular frequency corresponding to a wavelength λ_{on}, when the incoming signal travelling into input port with same wavelength as that of MR, switching take place i.e. signal get directed to drop port and when the signal in the input port is not of the same wavelength as that of MR i.e. the signal wavelength is off resonance λ_{off} with respect to the MR wavelength then the signal travels to through port. Multiple basic switching elements can be grouped together to perform a predefined switching function. By turning on/off the MRs an optical signal can be routed from input port to output port.

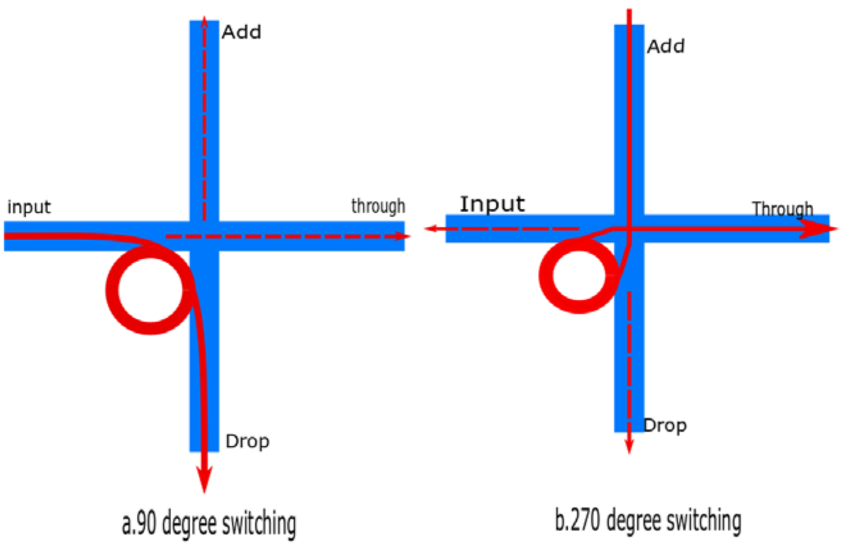

Figure 2: a) 90 degree and b) 270 degree switching in CSE.

In the CSE, there are four positions where MR can be placed. These positions of MR's provides flexibility in designing optical routers. The optical signal can switch from input ports to output ports depending on the position of MR. There can be *90 degree* and *270 degree* switch for each MR position in CSE. As illustrated in figure 2a, a MR is positioned closer to the input port, the optical signal from the input port will take a 90 degree turn to reach the drop port, which is conventional switching mechanism of a CSE. If the MR is positioned at the same position and the signal is coming in from the add port, which could be considered as an input port, the signal will be switched to the through port after taking a 270 degree turn inside a MR. This characteristic of CSE helps in switching signals from input port and add port to two different output ports. Therefore, the designer can use this special characteristic to lower down the number of CSE's used in an optical router.

In PSE, the MR are placed in between two parallel waveguides. It has got two input ports and two output ports. The two input ports are in port and add port while two output ports are through and drop ports. The incoming signal with wavelength λ_{on}, is switched to drop port and when input signal is off resonance λ_{off}, the signal reaches the through port. In PSE, the luxury of 90 degree and 270 degree switching is not available for PSE. The PSE's crosstalk is less as compared to CSE because there is no crossing involved.

Inside an optical router, an optical signal terminator is used to absorb the signal within the router. It acts as a sink for the optical signal and therefore it should be designed properly such that the optical signal should not be reflected back to create an unnecessary crosstalk.

Waveguide bendings is an important component in an optical router, required for connecting two elements in an optical router in presence of a physical bend in the design. It is basically an optical waveguide with two ports, input port and output port, but with a bend to provide a change in direction of optical signal travelling in a straight path with minimum scattering, distortion and losses. Waveguide bending radius plays a very vital role in signal distortion. Bending angle of an optical waveguide is usually 90 degree, 45 degree and 30 degree but it can be customized as per the requirement.

In an optical router there are waveguide crossings, which are unavoidable during the construction of the optical routers. An optical crossing element has four ports, two input ports and two output ports. The waveguide crossings in an optical router accounts for a major portion of crosstalk noise, hence the waveguide crossings must be used cautiously much as possible for a distortionless communication. Optical router like CRUX has the minimum of nine optical waveguide crossings and it has a very good SNR values compared to other optical router. Every optical crossing element leads to 0.12dB [1] of loss on a passing optical signal and therefore minimizing the waveguide crossing is a very important factor while designing an optical router.

As electrical components are connected together by an electric wire to form electrical networks, similarly, optical waveguides are the optical components which help in connecting these optical components together to form an optical network. Optical waveguides can be of different length according to the requirement. Optical waveguides are prone to insertion loss, propagation loss and scattering loss. The propagation loss is directly proportional to the length of the waveguide. The propagation loss of a waveguide is 0.17dB/mm [1]. In order to reduce propagation loss, it is suggested to make the area of the router as small as possible so that the waveguides used are minimum in number and thereby helping in lowering different losses.

2.1: Related works on Optical Routers

A 5x5 optical router has 10 ports, 5 input ports and 5 output ports. There are 4 bidirectional ports located at North, South, East and West directions of an optical router and other two ports are connected to the processor via optical to electronic interface(OE interface) and electronic to optical interface(EO interface), named as Injection and Ejection port. Router at the edge of an optical mesh network does not fully utilize 5x5 optical switching function hence a 4x4 optical router is used at the edges of a network. A 4x4 optical router contains 4 bidirectional ports located at North, South, East and West directions. The routing topology followed in an optical router is mostly XY routing apart from some routers which follow arbitrary routing topology. The 5x5 optical router proposed till date can be differentiated on the basis of routing algorithm, blocking/non-blocking, passive routing, number of MR's, number of optical terminator, number of optical waveguide crossing, number of optical waveguides and overall losses. Let us have a brief introduction about few state of the art optical routers.

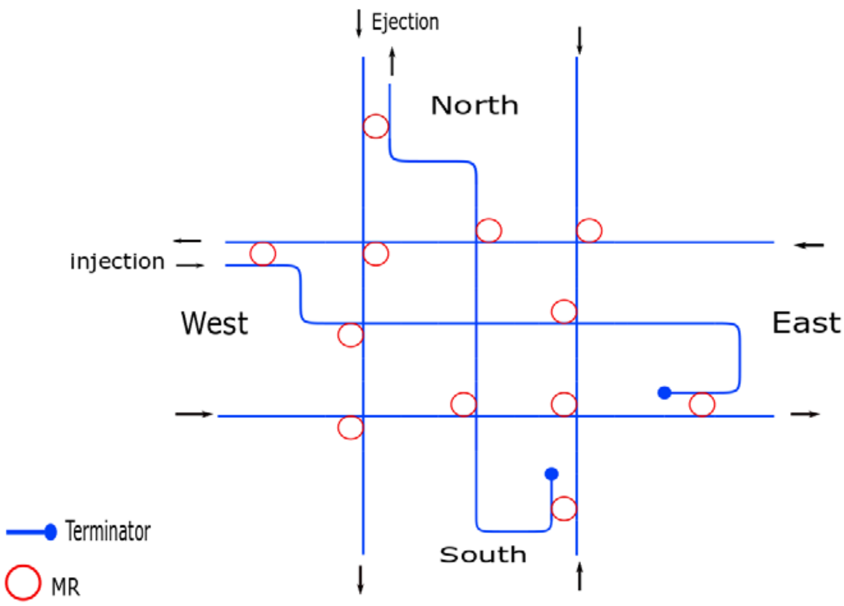

Figure 3: A 5x5 CRUX Optical Router.

1. **CRUX optical router**: It is a 5x5 non-blocking optical router in figure 3 with bidirectional port on North, South, East and West along with Injection and Ejection ports. It is composed of 12 MRs, 9 waveguide crossings and 2 optical terminators. It supports passive routing and follows XY routing algorithm i.e. each packet is routed in x direction until it reaches the same column of the destination and then along the y direction to reach the destination. At least one MR is turned on for every switching action except North-South, South-North, East-West, and West-East due of passive routing. CRUX takes the advantage of the PSEs to minimize the losses and waveguide crossings. For example, Injection port uses PSEs to reach West output and from North input to ejection port thereby reducing the number of waveguides and number of crossings. CRUX is the most efficient and compact 5x5 optical router. At any network size, at most three MR's will be powered on in any XY routing optical path in optical Mesh or Torus network. Its switching action is reduced for routing in Mesh and Torus optical networks.
2. **Cygnus optical router**: A 5x5 non-blocking optical router with five bidirectional ports include North, South, East, East and Injection/Ejection. Cygnus employs XY routing algorithm, passive routing algorithm. Cygnus contains 16 MR, 2 optical terminators and 13 optical waveguide crossings with total average loss of 0.78 dB [1]. Cygnus is not

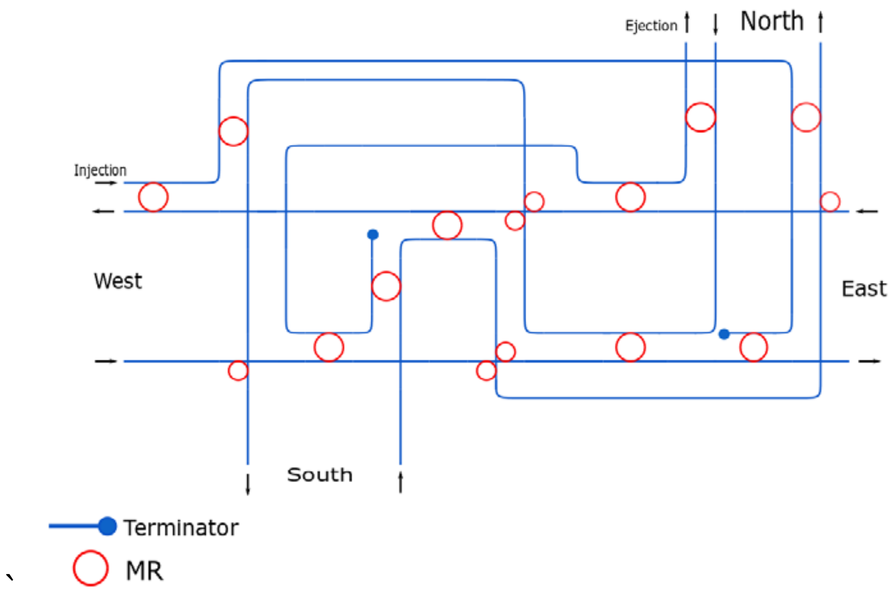

Figure 4: A 5x5 CYGNUS optical Router.

compact as CRUX and uses 4 more MRs. Cygnus requires 3 MR to be powered on for routing an optical signal in a mesh or torus network. As was the case in the CRUX router, Cygnus does not need any MR to be powered on while an optical signal travelling from North to South, South to North, East to West and West to East. Cygnus 5x5 optical router can be reduced down to 4x4 optical edge router which also inherits the passive routing property. The 4x4 optical router contains 8 MR, 8 optical crossing and the overall average loss is 0.66 dB [1].

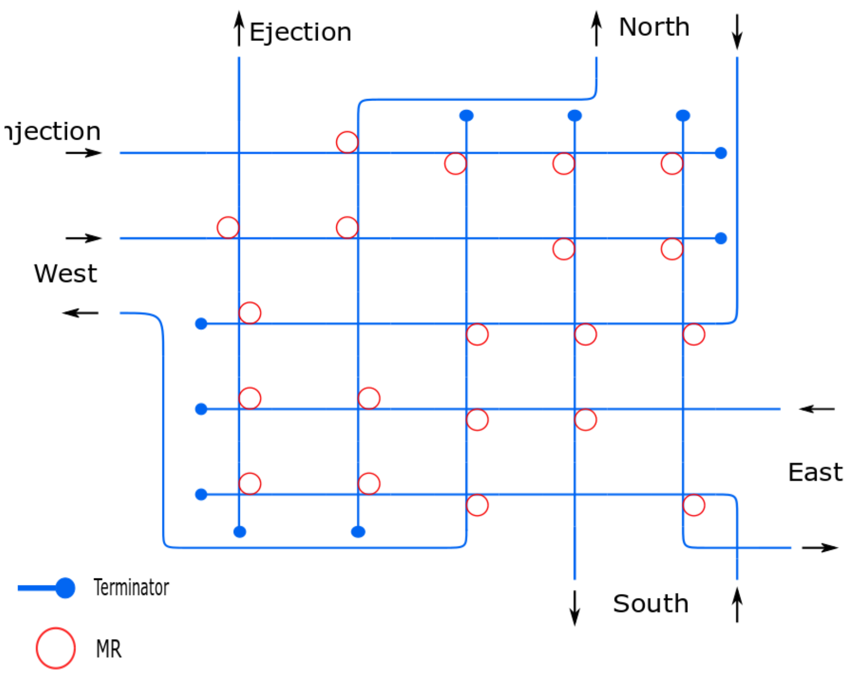

Figure 5: An optimized crossbar router

3. **Optimized Crossbar optical router**: It is a 5x5 non-blocking optical router which uses 20 MRs, 10 optical terminators and 26 waveguides crossings. It uses an arbitrary routing algorithm and is different from passive algorithms, one router has to be powered on for each switching action, which leads to more power consumption. The high number of waveguide crossings have led to the overall average loss of 1.15 dB [1] which is very high from the other proposed optical router.
4. Other proposed router designs are ODOR [1] with 12 MRs, 2 optical terminators and 19 waveguide crossing with overall loss of 0.87 dB. Min et al [1]. proposed a router with 15 waveguide crossings and microring resonators and no optical terminator.

2.2: Different Network Topologies of optical Network-on-Chip

The network topology defines how different nodes are connected and communicate with each other. Many different topologies have been proposed ,and among them, the '2D Mesh' and 'Torus' are most common topologies due to their grid type shape ,regular structure and compatibility with the two dimensional layout on a chip .

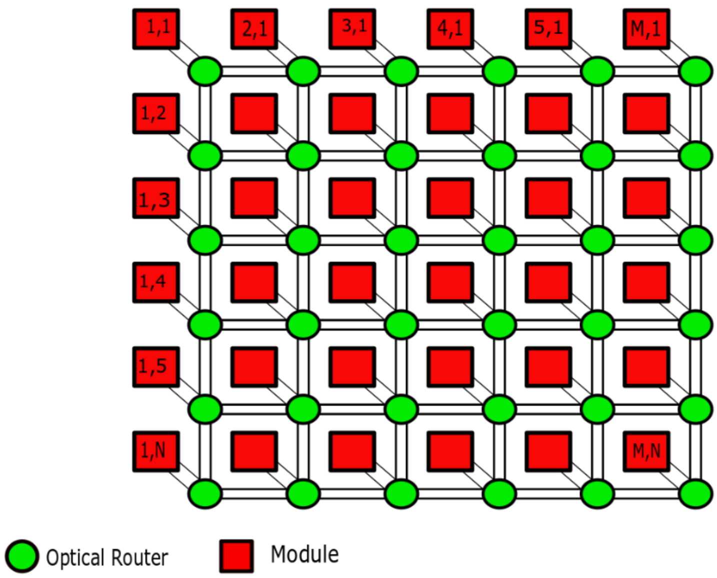

Figure 6: A MxN Mesh-Based Network Topology

1. **Mesh-Based Optical Network**: The figure 6 shows an MxN mesh based optical network [21]. It consists of processors cores, optical routers and optical waveguides which are connected through the mesh topology. In this network, every router, except those located at the network edges, is connected to four neighbouring routers and one

processor core. This topology allows the integration of a large number of cores in a regular shaped structure. In the mesh network, each core is assigned with coordinates as (x, y), where x<=M and y<=N. [15] In K. Feng, et al. studied the floor plan of mesh based and torus based networks. The study covered important design metrics for mesh based and torus based optical networks such as the number of waveguide crossing in the floor plan, number of paths and hops. When analysing the worst case and average case crosstalk noise in ONoCs, we need to consider the maximum as well as average hop length in each ONoCs architecture. The hop length is defined as the number of hops the packet should take from source core to reach the destination core indicated in MxN mesh based optical network using XY routing algorithm. The maximum hop length in the network is defined in equation (1) and average hop length in equation (2).

$$H_{Meshmax} = M + N - 2 \quad (1).$$

$$H_{Meshavg} = \frac{M + N}{3} \quad (2).$$

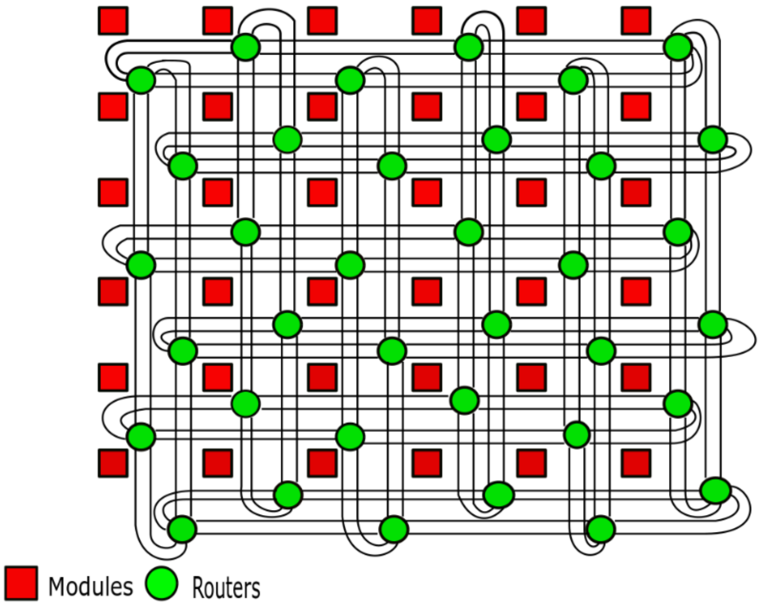

Figure 7: A folded torus based network topology

2. **Torus-Based Optical Network**: An MxN torus based network topology [21] is shown in figure 7. This topology is similar to mesh topology except that the edge router is connected to the opposite edge router using wrap around channels. As a result, better path diversity and load balance is achieved in torus-based network. Also the average

hop length in the torus network is smaller as compared to mesh-based network. From topological point of view torus has half the network diameter and 2 times the number of bisection connections compared to a mesh when accommodating the same number of processor cores. Compared with an unfolded torus topology, the folded torus benefits from better balanced hop latency and avoids extra energy consumption caused by wrap-around channels. Each processor core is assigned with coordinate as(x, y) where x<=M and y<=N. Folded torus network topology performs better than Mesh network topology with respect to average and maximum hop-length for XY routing algorithm.

2.3: Routing Algorithms.

Routing is the mechanism to determine the path that a packet transverses from the source node to destination node. Routing algorithms can be classified as deterministic or adaptive routings. In a deterministic routing technique, the path between the source core and the destination core is fixed regardless of the current state of the network. In contrast, an adaptive routing algorithm takes the network state into account when determining a routing path, resulting in the variation of routing path in time. In adaptive routing algorithms, if a certain link is congested it may choose an alternate path. Adaptive routing has the potential to support more traffic for the same network topology, but most of the proposed network-on-chip uses deterministic routing techniques due to their simplicity and low area overhead in router design.

1. Dimension ordered Routing Algorithm:

Dimension order routing also known as XY routing algorithm is a low complexity, distributed and deterministic algorithm without the need of a routing table. This algorithm routes packets first in the x-direction or horizontal direction towards the correct column and then in y-direction or vertical direction towards the destination. XY routing matches well with mesh-based or torus-based network. It never runs into deadlock and livelock. For a packet sent from the source processor (x_i, y_i) to the destination processor (x_j, y_j), the packet is first routed along the x-dimension until it reaches the router in the same column as the destination, $y_i = y_j$, and then it is routed along the perpendicular y-dimension towards the destination. The next hop on a path can be determined solely based on the destination address, resulting in reduction of control logic in the router as well as the length of the setup signal and ultimately the energy consumption of the router. It is worth mentioning that torus based networks using XY routing require additional deadlock-free technique to avoid deadlock. For example, in a wormhole-switching torus-based network, a deadlock-free virtual channel selection algorithm can be adopted to avoid the deadlock.

2. Turnaround Routing Algorithm:

Turnaround round is a routing algorithm for butterfly and fat-tree networks. It is also called the least common ancestor routing algorithm. In this routing technique, a packet is first route upstream until it reaches the common ancestor node of the source and the destination of the packet, and then, it is routed downstream to reach the destination. Turnaround routing is a minimal path routing algorithm, and it is free of deadlock and livelock. Furthermore, it is a low-complexity, adaptive routing algorithm without the use of any global information.

………………..

Chapter 3.

Challenges faced by ONoCs and its Mathematical Modelling.

ONoCs are made from various small optical components like MRs, optical waveguides, optical terminators and waveguide crossings etc, these components carry optical signals through them and are accounted for losses like insertion loss, propagation loss, thermal loss and crosstalks degrading the signal quality. The fabrication process used to develop optical components is SOI. SOI substrate is made of a thin silicon top layer separated from the silicon substrate by a buried oxide layer. Recent developments in nanoscale silicon photonics devices has substantially improved the feasibility of ONoCs. However, the intrinsic characteristics of photonic devices i.e. the thermal sensitivity is a potential issue in ONoCs. Chip temperature fluctuates temporally and spatially while the steady state temperature varies more than 30°C across a chip under normal operating conditions. As a result of thermo-optic effect, on-chip temperature fluctuation can affect the characteristic of photonic devices. Thermal effects is the potential cause of ONoCs degradation and can even lead to functional failure under large temperature variation.

Another key issue for WDM based ONoCs is the crosstalk noise. Crosstalk noise is also an intrinsic characteristic of optical components. Depending on the architecture of the network, crosstalk noise can be intensified due to the cumulative effect of all the optical routers in a network. Moreover, with the presence of a large number of wavelengths in one single waveguide can lead to increase in crosstalk noise as the changes in temperature leads to shift in resonant wavelength of the MRs. Fundamentally, the crosstalk noise can be classified into coherent crosstalk and incoherent crosstalk.

3.1: Crosstalk Noise in Basic Photonic Device

Silicon waveguide crossings and MR-based photonic switching elements has been used extensively in above mentioned optical routers and optical interconnection network architectures. Crosstalk noise and power loss caused by waveguide crossings plays an essential role in determining the network's performance degradation. Some efforts has been made to reduce crosstalk noise and power loss in a waveguide crossings. [15]T.

Fukazawa et al. fabricated a low loss elliptical intersection of Si photonic waveguide on a SOI substrate and indicated an insertion loss less than 0.1 dB at a wavelength of 1.55 um. [15]P. Sanchis, et al. offered the method of choosing the optimum crossing angle to reduce the crosstalk noise in waveguide crossings. They indicated widths between 400nm and 550nm, the optimum angle was always given for values around 60 degrees and 120 degrees but never for 90 degrees. [17] W. Bogaerts, et al. demonstrated a design that uses parabolically broadened waveguide and a double etch scheme to reduce the lateral refractive index contrast while still confining the light as much as possible in the crossing region. The work measured -0.16 dB crossing loss and -40 dB crosstalk. [13] X. Li, et al. demonstrated metal free integrated elliptical reflectors for waveguide turning and crossings. By employing four symmetric identical reflectors sharing an intermediate beam focused region in the direct waveguide crossing, crosstalk noise smaller than -30 dB and high transmission were achieved. An ultra-compact waveguide crossing with negligible crosstalk and insertion loss was proposed in which the intersection is filled with impedance matched metamaterial which effectively suppresses the diffraction of the guided mode in the crossing region. An insertion loss of as low as 0.4dB and crosstalk as low as – 40 dB or even smaller were obtained. In addition to waveguide crossing, several research groups have explored different microresonator structures.[13] F. Xia, et al. demonstrated compact, photonic wire based coupled resonator optical waveguide structure, including up to 16 racetrack resonators on SOI substrate and indicated a drop port loss less than -3 dB. The same group presented ultra-compact fifth-order ring resonator optical filters based on sub-micron silicon photonic wires. [13] Q. Li, *et. al* designed and fabricated a compact third-order coupled-resonator filter on the SOI platform with focused application for on-chip optical interconnects and obtained a drop port loss of less than 0.5 dB, an in band throughput-port extinction of 12 dB and an out-of-band drop rejection of 18 dB.

3.2: Crosstalk Noise in Optical Interconnection Networks

Compared to the amount of research dedicated to exploring the crosstalk noise issue at the photonic device level, only a few works have considered this issue at higher level in ONoC's. [15] J. Chan, et al. described a methodology to characterize and model basic photonic blocks, which can form full photonic network architectures, and used a physical layer simulator to assess the physical-layer and system level performance of a photonic network. Also a simulation environment, called Phoenix Sim, was proposed for the design, analysis and optimization of optical interconnect networks. [13] D. Ding et al presented GLOW, a hybrid global router, to provide low power opto-electronic interconnect synthesis, while considering thermal reliability and various physical design constraints such as optical power, delay and signal quality. [17] L. Bai et al proposed a crosstalk aware routing algorithm to relieve the crosstalk noise problem in Benes ONoC's. The fundamental limits for the number of WDM channels and power per channel when using building blocks that include silicon waveguides, silicon microring modulators and filters were described by K. Presto [17] et al. Y. Xie, analysed the worst case crosstalk noise and SNR in mesh based ONoC's using an optimized crossbar optical router. Furthermore, the CRUX optical router, which is a compact high-SNR optical router was proposed to outperform the SNR in mesh-based ONoC's. In the same work, it was proved that the worst case SNR link in mesh-based ONoC's is not the longest optical link, which suffers from the maximum power loss in the network. M. Nikdast, et al. proposed a formal analytical method to systematically study the worst-case crosstalk noise and SNR in folded torus based ONoCs using arbitrary optical routers. The worst case SNR link candidates in arbitrary folded torus based ONoC's were found and analysed.

3.3: Analytical Modelling of Crosstalk Noise of Basic Optical Device.

Basic photonic components have been widely employed to construct optical routers and ONoCs. The expensive fabrication process and the need for compact optical routers requires integrating these basic optical components on a single silicon layer. As a result, due to the mode coupling in the optical signals, such devices transmits optical signal while imposing power losses and crosstalk noises. For instance, in an ideal waveguide crossing which consists of two orthogonal waveguides, the latitudinal and longitudinal waveguides are in the same plane. In a perfect crossing arrangement, optical modes propagate with 100% transmission from input waveguide to an output one on the opposite side of the crossing intersection, with no reflection and with 0% transmission to other output. However, an ideal crossing is impossible due to the coupling of four branches, or ports, at the intersection in terms of resonant cavity at the centre. The resonant nodes which are excited from the input port can be prevented by the means of symmetry from decaying into the transverse ports, therefore the crosstalk noise can be eliminated. Nevertheless perfect crossing cannot be attained.

Parameter	**Notation**
Crossing Loss	L_c
Propagation Loss	L_p
Power Loss per CSE in the OFF state	L_{c0}
Power Loss per CSE in the ON state	L_{c1}
Bending Loss	L_b
Power Loss per PSE in OFF state	L_{p0}
Power Loss per PSE in ON state	L_{p1}
Crossing's crosstalk coefficient	K_c
Crosstalk Coefficient per PSE in the OFF state	K_{p0}
Crosstalk Coefficient per PSE in the ON state	K_{p1}
Optical terminator's reflectance coefficient	K_t
Crossing's back-reflection coefficient	K_r

Table 1: Parameter description for optical elements [16] [17].

The waveguide crossings illustrated in figure 1, consist of an input port and three output ports, which are out1, out2 and out 3. When two optical signals go through a crossing simultaneously, crosstalk will be created at the crossing intersection. Moreover, a small portion of light will be reflected back on the input port. [16] [17] Given, P_{in} as the signal power at the input port, the crossing loss from the input port to the output port 'out1' and the generated crosstalk noise at the 'out2' and 'out3' output ports in equation (3) and equation(4), respectively. Moreover, the reflected power on the input port, P_{Rc}, is calculated in equation (5). In these equations, P_{out1}, P_{out2}, and P_{out3} respectively indicate the output power at out1, out2, and out3 output ports. The basic function of an optical terminator is to avoid light reflecting back on the transmission line. The reflected power, P_{Rt}, of the optical terminator can be written as equation (6).

$$P_{out1} = L_c P_{in} \quad (3).$$

$$P_{out2} = P_{out3} = K_c P_{in} \quad (4).$$

$$P_{Rc} = K_r P_{in} \quad (5).$$

$$P_{Rt} = K_t P_{in} \quad (6).$$

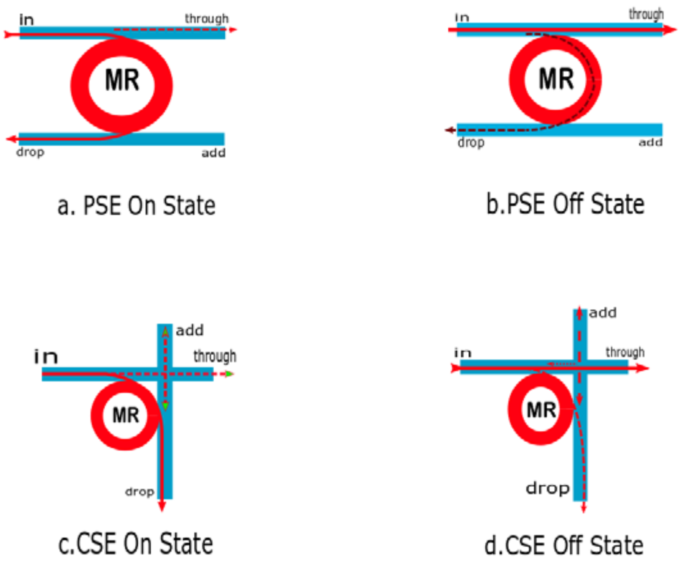

Figure 8: ON and OFF states of PSE and CSE.

The PSE in figure 8 is a structure consisting of a MR located between two parallel waveguides. Basic optical switching elements can be powered on and off according to the following way.

1. OFF state: The signal wavelength (λ_s) of the optical signal is different from the resonant frequency of the ring (λ_{off}). The input signal propagates from input port to the through port when the microresonator is powered off.
2. ON state: The switch is turned on by injecting an electrical current into the p-n contacts surrounding the rings or changing the temperature using the metal-plate based thermal heating. The resonance frequency (λ_{on}) of the microresonator shifts so that the light ($\lambda_S = \lambda_{on}$), now on resonance, is coupled into the ring and directed to the drop port, thus causing a switching action.

The passing loss and the cross talk noise at the through and drop ports of the PSE in the OFF state are calculated in equation (7) and equation (8) respectively. Moreover, when the PSE is in the ON state, equation (9) calculates the crosstalk noise at the through port, while equation (10) calculates the drop loss of the PSE. In this equation, P_T is the output power at the through port and P_D is the output power at the drop port.

$$P_{T\ pse,off} = L_{p0}\ P_{in} \quad (7)$$

$$P_{D\ pse,off} = K_{p0} P_{in} \quad (8)$$

$$P_{T\ pse,on} = K_{p1} P_{in} \quad (9)$$

$$P_{D\ pse,on} = L_{p1} P_{in} \quad (10)$$

Considering the waveguide bending, the output power of the waveguide can be calculated based on equation (11).

$$P_{out} = L_{b}\ P_{in} \quad (11)$$

The CSE consists of a waveguide crossing and MR placed next to the intersection of the crossing. The power losses and crosstalk noise analytical models of the CSE can be derived based on PSE and the waveguide crossing. Considering the proposed analytical models of the PSE in the OFF state and the waveguide crossing, the output power at the through port, P_T, the drop port, P_D, the add port, P_A and the reflected power on the input port, P_R, of the CSE in the OFF state has been calculated in equations (12), (13), (14), (15) respectively.

$$P_{T\ CSE,off} = L_{c0} P_{in} = (L_{p0} L_c) P_{in} \quad (12)$$

$$P_{D\ CSE,off} = (K_{p0} + L_{p0}^2\ K_c)\ P_{in} \quad (13)$$

$$P_{A\ CSE,off} = K_c\ L_{p0} P_{in} \quad (14)$$

$$P_{R\ CSE,off} = L_{p0}^2 K_r P_{in} \quad (15)$$

Also, when the CSE is in the ON state, the output powers can be calculated using the analytical models of the PSE in the ON state and the waveguide crossing as described by equation (16) to equation (19)

$$P_{T\ CSE,on} = K_{p1}(L_c\,(1 + K_c L_{p1}) + K_r L_{p1} K_c)\ P_{in} \quad (16)$$

$P_{D\ CSE,off} = L_{c1}P_{in}$ (17)

$P_{A\ CSE,on} = K_{p1}(K_c (1 + K_cL_{p1}) + K_rL_{p1}K_c)\ P_{in}$ (18)

$P_{R\ CSE,off} = K_{p1}^2K_rP_{in}$ (19)

According to figure 8, the power loss of the CSE in the OFF state, L_{c0}, can be calculated based on the models of the waveguide crossing and the PSE in the OFF state as $L_{p0}L_c$, in which L_{p0}corresponds to the passing loss caused by the MR and L_c is the crossing loss of the waveguide crossing. When the CSE is the ON state, the power loss,L_{c1}, can be calculated by considering the models of PSE in the ON state and the waveguide crossings, which results in $L_{p1}(1 + K_{p1}^2K_c) + K_{p1}^2K_c$. Based on this equation, since the crosstalk coefficients are very small numbers (K_iK_j □= 0), L_{c1} can be approximated byL_{p1}. Different sources of power losses and crosstalk noise in the CSE can be similarly described.

3.4: Thermal Model of Optical Network-on-Chip.

ONoCs offers a new approach to empowering ultra-high bandwidth with lower power consumption, there are also voices of concern about the reliability of optical interconnection for on-chip applications. From [3], an investigation of thermal issues of on-chip optical interconnects shows that, with the consideration of internal regulation power, optical interconnects may not have advantages in power efficiency as compared with their electrical counterparts. More device-level investigations of thermo-optic effect has been carried out in literature. As a result of thermo optic effect, material refractive index changes with temperature. For example, the thermo-optic coefficient of silicon is on the order of 10^{-4} /K. This will cause changes in the refractive index of silicon based MRs to be about 50-100 pm/K, which is non-negligible in practical use. As a widely used device in ONoCs, MRs performs wavelength selective optical switch or a modulator, the undesired wavelength mismatch caused by temperature variation will result in additional optical power loss. Thermal tuning by local micro-heaters is an alternative solution to compensate for the temperature dependent wavelength shift of MR. Tuning efficiency in current technology is in order of several mW/nm. Other optical link modules such as laser source and optical receivers are also sensitive to temperature variations. Investigations of temperature sensitivity of Vertical Cavity Surface Emitting Laser (VCSEL) shows that the temperature dependent wavelength shift is comparable to or even larger than that of MR. Furthermore, because of the mutual shift between lasing wavelength and peak material gain wavelength under temperature variation, VCSEL power efficiency degrades seriously at high temperatures. There has been investigations of temperature dependent behaviour of Ge-based photodetectors. Temperature sensitivity of the whole network-on-chip should be considered during ONoCs architecture design and power efficiency evaluation.

ONoCs relies on optical signal to communicate payload data as well as control information among processor cores and memories. In different ONoCs architectures, optical signal are transmitted through different optical links between sources and destinations. Most ONoCs architectures employ photonic devices which can be integrated with existing CMOS based processor cores either through CMOS compatible fabrication processes or bonding technologies. Despite the architectural diversity, an optical link in ONoCs is generally composed of an optical transmitter, an optical link and optical receiver. The optical transmitter can convert electrical signals into optical signals by directly modulating the driving current of the VCSEL or using an optical modulator. On the optical path between the transmitter and receiver, multiple switching elements switch optical signals in stages onto a series of optical waveguides until reaching destination. MR-based add drop filter has been widely used as the switching element to perform the switching function in ONoCs.

On chip Temperature Variation and Thermo Optic Effect.

The absolute temperature and temperature fluctuations across the chip has been a major concern in chip design and packaging because a changes in temperature could cause performance degradation and even functional failures in CMOS circuits. Transient thermal analysis shows that the chip temperature responds to power changes quickly at beginning and takes a relatively long time to reach the steady state. Steady-state temperature of the chip also varies spatially because of the non-uniform power densities across the chip as well as the limited thermal conductivity of the die and packaging material. For example, in Intel Itanium processor which is under stringent thermal management, while some parts of the chip can be maintained at relatively low temperature of 60◌Ĉ, the other part of chip can still reach about 88◌Ĉ [3]. In general the maximum junction temperature on chip is 25◌ Ĉ higher than average, and chip temperatures can vary by more than 30◌ ̊C [3] across the chip under typical conditions. As a result of thermo-optic effect, material refractive index is temperature dependent and follows equation (20), where n_0 is the refractive index at room temperature, dn/dT is the thermo-optic coefficient of material, and ΔT is the temperature variation.

$$n = n_0 + \frac{dn}{dT}\Delta T \qquad (20)$$

Since refractive index is an important device parameter, the thermo-optic effect will cause changes in device characteristics. For a MR, the resonance wavelength is directly governed by an effective refractive index and the resonance wave-length, red shifts with increasing temperatures.

a. Thermal sensitivity of Optical Transmitters.

Optical transmitters converts electrical signal into an optical signal by either directly modulating the driving current of VCSELs or using an optical modulator. Optical modulators can be used to indirectly modulate the optical signal outputted by VCSEL or off-chip lasers sources. VSCEL's are a good candidate for on-chip laser source because of low power consumption, high modulation bandwidth and manufacturing advantages. The emission wavelength of VCSEL, λ_{VCSEL}, is determined by cavity resonance, where n_{ave} is the spatially averaged refractive index of the laser cavity, l_{Vcsel} is the cavity length, and m_{VCSEL} is the resonance order. The temperature dependent wavelength shift of VCSEL emission is mainly governed by the change of n_{ave} under temperature variations.

$$l_{VCSEL} \cdot n_{ave} = m_{VCSEL} \cdot \frac{\lambda_{VCSEL}}{2}. \qquad (21)$$

For VSCELs in the emission wavelength range 800 – 1000 nm, the temperature dependent wavelength shift of the cavity resonance is typically found to 0.07nm/◌Ĉ[3] and the shift of the peak material gain wavelength is about 0.32nm/◌ Ĉ [3]. Beside the temperature dependent wavelength shift, the power efficiency degrades with increasing temperature as a result of thermal effects on the threshold current and slope efficiency. Because of the different temperature dependent shifts of the cavity resonance and peak gain, a mutual shift between the lasing mode and gain spectrum occurs when temperature changes. The misalignment causes the threshold current I_{th} of VCSEL to increase with temperature T following approximate shaped curved shown by equation(22) where α is the minimum threshold current, β is a coefficient related to gain properties, and T_{th} is the threshold temperature at which cavity resonance is spectrally aligned with peak gain.

$$I_{th} = \alpha + \beta\,(T - T_{th})^{2} \tag{22}$$

If the driving current is above the threshold, the output power will increase approximately linearly with driving current. Slope efficiency is an incremental increase in output power for an incremental increase in driving current. The slope efficiency decreases approximately linearly with an increasing temperature and can be expressed by equation (23) where ε is the slope efficiency at 0◌Ĉ and γ is positive coefficient.

$$s = \varepsilon - \gamma.\, T \tag{23}$$

From [3], when the temperature changes from room temperature to 80◌ Ĉ, the slope efficiency decreases from 0.36 to .23 mW/mA, and the maximum emission power decreases from 4 to 1.5 mW correspondingly.

b. Thermal Sensitivity of Switching Elements.

On the optical path between the transmitter and receiver, multiple switching elements switch optical signal in stages onto a series of optical waveguides until reaching their destinations. MRs of different structures has been widely used as the switching functionality of a ring based MR. A MR has two distinctive states, on state and off state. In the on state, the resonant wavelength of the MR is the same as the wavelength input signal and optical signal will be coupled to drop port. In the off state the MR shifts to different resonant wavelength from the one which carried the input optical signal, and the optical signal will propagate directly to through port. ONoCs set the resonant wavelength of the MR according to network routing information to establish optical paths between transmitters and receivers. The peak resonant wavelength λ_{MR} of MR obeys the relationship in equation (24), where l_{MR} is the one round length of the ring, m_{MR} is an integer indicating the order of the resonance, and n_{eff} is the effective refractive index of the waveguide mode involved in the resonance.

$$l_{MR}.\ n_{eff} = m_{MR}.\ \lambda_{MR} \tag{24}$$

With a constant l_{MR} and m_{MR} the peak resonant wavelength λ_{MR} will change in proportion with n_{eff}. Since n_{eff} changes with the temperature, the peak resonant wavelength will also vary with temperature. Both theoretical analysis and experiments confirm a linear relationship between resonant wavelength shift and temperature. The linear relationship can be defined as in equation (25) where ρ_{MR} is defined as the microresonator temperature-dependent wavelength shift coefficient, λ_{MR_0} is the resonant wavelength at initial temperature, σ_{eff} is the thermo-optic coefficient (dn/dT) of the effective index, and n_g is the group index of the wave guide.

$$\rho_{MR} = \frac{\lambda_{MR\_0}}{n_g}.\ \sigma_{eff}\ . \tag{25}$$

An ideal lossless MR would confine light indefinitely, but intrinsic loss always exists in any physical implementation of cavities. The deviation from ideal condition is defined by the quality factor (Q), which is proportional to the confinement time of the cavity. The total quality factor of a ring based MR used in figure 7 is defined by equation (26), where λ_{MR} is the resonant wavelength, 2δ is the 3dB bandwidth of the drop port power transfer spectrum, κ_e^2 is the fraction of power coupling between the drop port and the ring and κ_p^2 is the power loss per round trip of the ring. MR with Q can range from 1500 to 100000.

$$Q = \lambda_{MR} / 2\delta = (2\pi n_g l_{MR}) \ / \ (\lambda_{MR}(\kappa_e^2 + \kappa_d^2 + \kappa_p^2)) \tag{26}$$

MR has a Lorentzian power transfer function which is peaked at the resonant wavelength λ_{MR}. For optical signal with wavelength λ_s, the drop power function can be expressed as equation (27). When $\kappa_e^2 + \kappa_d^2 >> \kappa_p^2$, nearly full power transfer can be achieved at the peak resonance point, and MRs will exhibit a low insertion low. Physical Implementation shows that the insertion loss of a MR can be practically lowered to 0.5 dB.

$$P_{drop}/P_{in} = ((2\,\kappa_e\,\kappa_d)/(\kappa_e^2+\kappa_d^2+\kappa_p^2))^2 \cdot (\delta^2/((\lambda_s-\lambda_{MR})^2+\delta^2)) \quad (27)$$

According to (27) a deviation from the peak resonant wavelength would result in more power loss at the drop port especially for a high-Q MR. For a MR at 1550nm wavelength range, if Q is on the order of 10^4, a 10°C temperature change would make the power spectrum shift about 0.5 nm and resulting in power loss variation of about 16 dB for optical signal carried by 1550 nm wavelength. The loss variation would increase to 22 dB for 20°C temperature change and 26 dB for a 30°C temperature change [13]. For ONoCs requiring multiple switching stages on each optical link, the problem can become more serious as multiple switching elements could reduce the optical signal strength significantly.

c. Thermal Sensitivity of Optical waveguide.

ONoCs use optical waveguides to connect transmitter, switching elements, and receiver together to form optical links. Silicon- based waveguides can be fabricated on SOI substrate with silicon slab on top of buried oxide layer which prevents optical mode from leaking into the substrate. The cross-section of a single mode waveguide can be designed to be 510 nm X 226 nm with minimum propagation loss and group velocity dispersion [13]. As a result of thermo-optic effect, both the waveguide propagation loss and latency are temperature dependent.

1. Propagation loss variation in optical waveguide: The silicon core of a waveguide has a negligible absorption of energy and the propagation loss is dominated by sidewall roughness scattering. Propagation loss in a straight optical waveguide can be estimated by equation (28) where ε is a parameter regarding in interface roughness, k_0 is free space wavenumber, β is the modal propagation constant, h is the transverse propagation constant in waveguide core, Φ is the refractive index difference between the waveguide core and cladding material, and $E_S^2/\int E^2 \mathrm{dx}$ is normalized electric field intensity at the waveguide core/ cladding interface.

$$L_{WG} = \frac{4\varepsilon^2 k_0^2 h}{\beta} \cdot \frac{E_S^2}{\int E^2 dx} \cdot \Phi^2 \quad (28)$$

As shown in equation (28) the waveguide propagation is proportional to the refractive index difference between the core and the cladding. Because of the different thermo-optic coefficients (dn/dT) of the core and the cladding, the propagation loss will also change with operating temperatures along the waveguide which is uniformly distributed between T_0 and $T_0 + \Delta T$, the corresponding waveguide propagation loss variation is expressed in (29), where L_{WG_0} is the propagation loss at room temperature T_0. σ_c and σ_d are defined as thermo-optic coefficients of the waveguide core and cladding material, respectively. For an optical waveguide with Si core and SiO_2 cladding, the refractive index difference Φ is approximately equal to 2.

$$L_{WG}=L_{WG\_0}.\,(1+ \frac{\sigma_c - \sigma_d}{\phi}.\Delta T + \frac{(\sigma_c - \sigma_d)^2}{3\phi^2}.(\Delta T)^2) \quad (29)$$

Based on equation (29) the propagation loss variation on Si/SiO_2 waveguide is about 0.22 %, from [13]. Waveguide propagation loss is less sensitive to temperature compared to insertion loss of high-Q switching elements.

2. Latency variation in optical waveguide: For an optical waveguide with a length of l_{WG}, the light latency D_{WG} is defined as in equation (30), where c is speed of the light in vacuum, and n_g is waveguide group index.

$$D_{WG}= \frac{l_{WG}}{c}\,.\,n_g \quad (30)$$

Because of the thermo optic effect in n_g the waveguide latency is also temperature dependent. High latency variation would lower data rate.

e. Thermal sensitivity of Optical receivers.

Optical receivers use photodetectors for optical to electrical conversions. Most photo detector designs use Ge as the absorbing material because of the high absorption coefficient of Ge in the near infrared spectrum as well as its compatibility with CMOS fabrication process. The photodetectors converts the optical signal into electric current and subsequent TIA-LA circuits then convert electric current to logic level. The concern for the temperature-dependent behaviours of Ge based photodetectors is potentially due to the excessive dark current under high operating temperature. From [3],” Studies show that the dark current of 10um x 10um Ge-on-SI photodetectors increases from 20 to 192 nA when temperature changes from room temperature to 86° C, while the receiver sensitivity does not have obvious change. In high speed optical receivers design 1uA is generally regarded as the upper limit of the tolerable dark current. Although the dark current of the photodetectors increases with temperature, it is still sufficiently low so as not to degrade the receiver’s performance even under high operating temperature.”

Note: All the equations have been taken from documents referenced in [3],[13],[14],[15], [17].

....

Chapter 4.

Introduction to Simulation tools.

In this dissertation, two simulation tools, OTEMP [3] and CLAP [2], were being used to simulate and analyze the result. These two tools are designed in C++ environment which allows the users to model an optical routers and simulate them to analyze the crosstalk, SNR and thermo-optic effect on optical routers and optical networks. These tools were introduced by researchers of Big Data Systems Labs and Optics Labs at Hong Kong University. These tools are optimised for faster simulation and quick results. Let us have a brief introduction about these simulation tools.

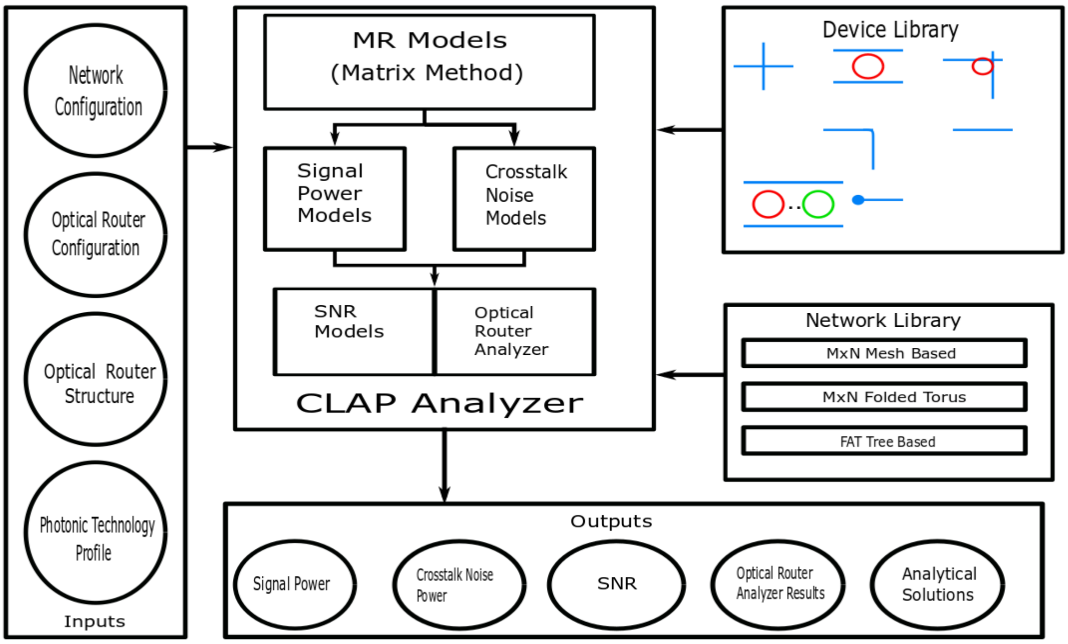

Figure 9: CLAP Block Diagram [2].

4.1: CLAP- Crosstalk and Loss Analysis Platform

CLAP tool [2] is implemented in C++ and analyses both coherent and incoherent crosstalk noise, propagation loss and SNR in optical networks and optical routers based on WDM or a single wavelength. CLAP has comprehensive library of photonic devices to construct arbitrary optical routers and optical networks, including detailed MR model, I/Os, waveguide crossings, waveguide bendings, waveguides, and optical terminators, PSE, CSE and filter elements with photodetectors. Mesh-based, folded-torus-based and fat-tree-based optical networks are predefined in network libraries. CLAP can be extended to include more optical network architectures. CLAP analyses the power loss, crosstalk noise power, and SNR in free-scale arbitrary optical interconnects and optical routers at the system level.

From figure 9, CLAP's internal structure includes inputs, a CLAP analyser, outputs, a device library and a network library. The analytical models in CLAP analyser are used for calculations at the network level as well as the optical router level. CLAP considers four input files: *Network Configuration, Router Configuration, Router Structure, and Technology Profiles*. A careful and simple text based syntax is considered for different input definitions in CLAP. *Network Configuration* consist of the network size, chip size, and communication pattern among the processor cores, while *Router Structure* includes the definition of the optical router structure. Different configurations of the optical router as well as the input power at the ports of the router can be defined in *Router Configuration*. CLAP considers different sets of parameters for different optical routers. Hence, the folder *Technological profiles* consist of different photonic device parameters like power loss values, reflectance coefficient, crosstalk coefficients, MR diameter, and the injection laser power. The analytical model for the optical network in CLAP is based on matrix analysis. Based on the proposed analytical models, the signal power, crosstalk noise power, and SNR at the destination of a specific optical signal, defined by the user, can be analysed in CLAP analyzer. Furthermore, the optical router analyzer helps in analysing the worst case as well as the average power loss and crosstalk noise in an optical router under various configurations. CLAP is capable of analysing the propagation loss at device, router and network levels. It is worth mentioning that the dimension ordered routing technique, also known as XY routing algorithm, is used in mesh based and folded-torus-based network, while the optical turnaround routing algorithm is considered for fat-tree-based network in CLAP.

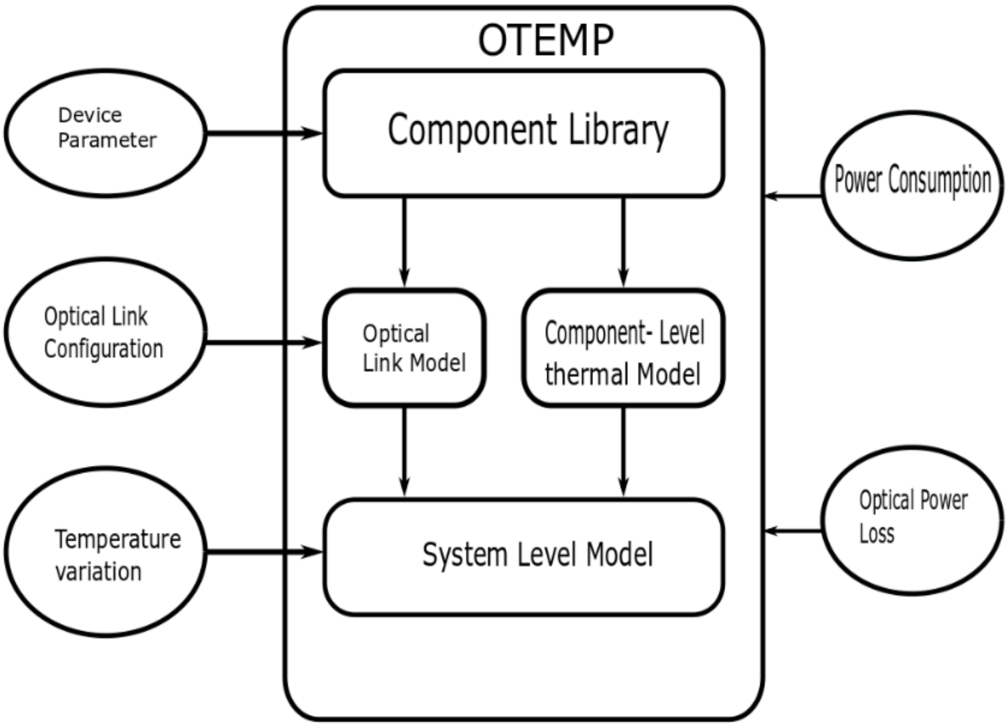

Figure 10: OTEMP Block diagram [3].

4.2: OTEMP: Optical Thermal Effect Modelling Platform

Optical interconnects (including on-chip and on-board optical interconnect) is an emerging communication technique that can potentially offer ultra-high communication bandwidth and low latency to multiprocessor systems. Thermal sensitivity is an intrinsic characteristic as well as potential issue of photonic devices used in optical interconnects. Chip temperature fluctuates spatially, and steady state temperature can vary significantly across a chip under typical operating conditions. As a result of thermo-optic effect, temperature variations can potentially cause power efficiency degradation. Optical interconnects thermal model at system level are required to fully understand these challenges. OTEMP [3] is used for both WDM-based and single-wavelength based optical links in optical interconnects. OTEMP is based on system-level optical interconnect thermal models. OTEMP is a C++ based program to analyze thermal-aware power consumption as well as the optical power loss for optical links under temperature variations. The inputs to this tool include the photonic devices parameters, the optical links configurations, and the temperature range. The component library of OTEMP includes optical link components such as BOSE (Basic optical switching element), BOME (basic optical modulation element), and BOFE (basic optical filter element). OTEMP models the thermal effects in component level and then arrives at the system-level thermal model according to the relationship between different components in an optical link. OTEMP takes two simple input text files: *parameter file* and the *configuration file*. The *parameter file* contains the list of parameters of photonic devices like the operating temperature, propagation loss, number of crossings, link length, sensitivity etc. The *configuration files* contains the configuration for WDM- based optical link includes choosing to use on-chip or off-chip VCSEL as the laser source, choosing whether to use BOME for modulation or direct- modulated VCSEL, the number of wavelength, the switching mechanism for BOSE, number of active and passive switching element, the quality factor of the MRs used in WDM-based optical link. The output of OTEMP includes worst case and average case power consumption with or without thermal based adjustments. If using on-chip VCSELs as the laser source, the total power consumption is equal to the on chip power consumption. If using off chip VCSELs as the laser source, the main concern is with the on-chip power consumption. The output file includes both the total power consumption and on chip power consumption. The worst case analysis is conducted among all possible thermal maps where the maximum temperature is T_{max} and the minimum is T_{min}. The average analysis considers all possible temperature conditions and gets the average power consumption based on uniform temperature distribution from T_{max} to T_{min}.

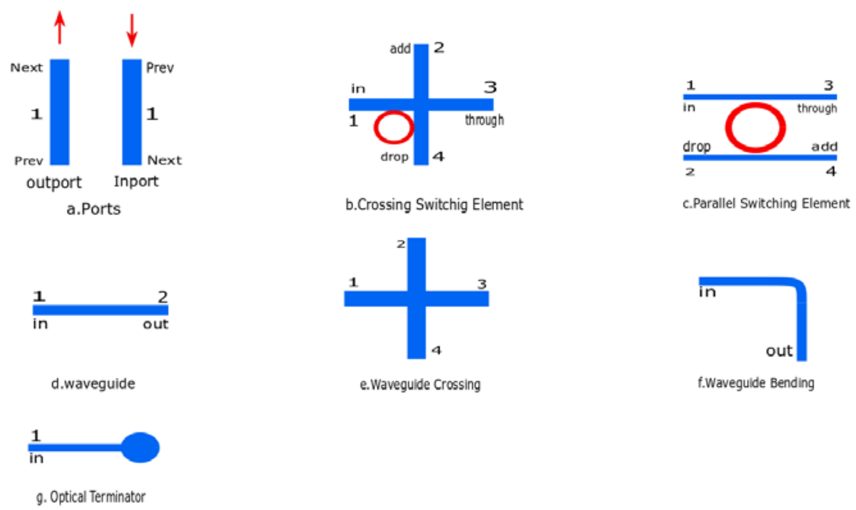

Figure 11: Optical elements Used in CLAP

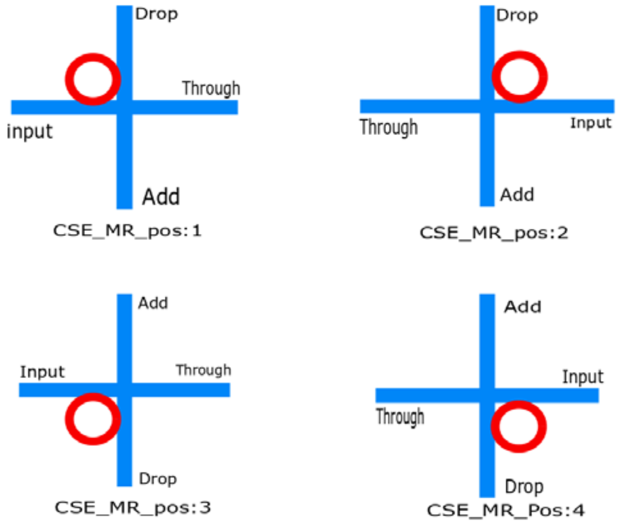

Figure 12: MR positions in a CSE

4.3: Router Modelling using CLAP Simulation Tool.

The first objective was to model an optical router with the help of CLAP tool [2]. CLAP tool provides the user with the procedure to design optical routers, i.e. defining each optical component like optical waveguide, CSE, PSE, optical terminator, waveguide crossing, optical ports and wave guide bendings. All the optical elements can be defined and connected together in a simple text file mentioned in section 4.1 and the text file is given as an input to the CLAP simulator and the simulation results provides coherent and incoherent crosstalk, SNR and signal power. The optical elements used in the CLAP tool is shown in figure 11. These optical elements must be defined according to the norms mentioned in the CLAP tool's user manual [2]. The norms provides a definition of each elements that must be declared specifically for each optical elements while designing an optical router. A brief introduction to all the input files has been provided from the CLAP manual [2].

a. Technological Profile.

The users of the CLAP simulation tool can define a set of required parameters for the basic optical elements and switching elements as a photonic technological profile. A set of photonic device parameters could be defined as a text file following the format Technology Profile_<tech_profile_number>.txt. Multiple device parameters could be defined for different sets of routers. The user can define the power loss values, crosstalk coefficients, reflectance coefficients, waveguide dimensions, the micro resonator's diameter, and the injection power in the text file. The table below gives the list of the photonic technological profiles with the values used.

Parameter for Basic Optical Elements	Notations	Values
Number of wavelengths	WDM	64
Crossing Insertion Loss	L_c	O.04 dB
Crossing Crosstalk Coefficient	K_c	40 dB
Crossing Back Reflectance Coefficient	K_r	0 dB
Parallel Switching Passing Loss	L_{pse_off}	0.2 dB
Parallel Switching Drop Loss	L_{pse_on}	0.33dB
Parallel Switching Crosstalk Coefficient in OFF state	K_{pse_off}	20.87 dB
Parallel Switching Crosstalk Coefficient in ON state	K_{pse_on}	8.86dB
Optical terminator Black reflectance coefficient	K_t	50dB
Waveguide Bending Loss	L_b	0.005dB
Propagation Loss	L_p	0.247dB/cm
Wavelength polarization Loss	L_{pol}	0dB
Coupling loss	L_{cpl}	1dB
Micro-resonator dimension	MR_Dim	10 um
Waveguide Width	WGD_width	2 um
Input Optical Power	P_{in}	0dBm
Micro-resonator Quality Factor	MR_Q	9000
Free Spectral Range	FSR	10
Micro-resonator-wavelength-Range	MR_wvlgth_range	1550nm

Table 3: Parameter File description [2].

Table 3 provides information about the values for each parameter used while simulating the modelled optical router.

a. Optical Router Configuration

The optical router analyzer function helps the user to analyze the signal power, crosstalk noise power, and SNR in the arbitrary optical routers. The router structure is defined in *Router_Structure_Definitions.txt* file, the user can define the optical router configuration in the *Router_Configuration.txt* input file. In this text file, the user can define the input powers at different input ports and the order of the crosstalk analysis and configure the optical router by setting pairs of input/output ports. The order of crosstalk noise analysis is the degree of the crosstalk noise coefficient in the analyses, if the crosstalk order equals two, the analyzer will compute all crosstalk noise coefficients to the degree of two in the router. The user should follow the syntax described below.

b. Network Configuration

The user can configure the network in the input text file called the *Network_configuration.txt*. The network size, the chip size, and the communication pattern among the processor cores can be defined in this input file. In CLAP, there are three interconnect topologies, mesh based, folded torus based and fat tree based network architectures. In every architecture, each processor core can be addressed using coordinates, the user can define the communication pattern among different processor cores in the network.

c. Top Level Configuration

When all the parameters for device parameters, router structure and network structure have been set up, the user can start using CLAP by selecting an optical architecture as well as the coordinates of the source and the destination of an optical link under analysis in the input file called *input.txt* as following

d. Output of CLAP tool.

CLAP indicates the signal power, crosstalk noise power, and SNR at the destination of the defined optical link either on screen or in an output text file. CLAP also generates the analytical equations used for analysing the signal power and crosstalk noise power in optical interconnects.

……………

Chapter 5.

Case Study of Today's Optical Network-on-Chip.

Presently, ONoCs has not been able to make early in-roads in becoming the core interconnect of the present on-chip architecture but it is being used in hybrid interconnect architectures [8] where both electronic and optical interconnects are used to route the data packets. The optical interconnects are used when the requirement of bandwidth and speed is high in order to process large data packets. The implementation of hybrid interconnect technology [8] has shown major improvements packet routing activities.

ONoCs can be implemented as mesh-based network topology, folded torus-based network topology, and fat tree based network topology. The main backbone of an optical network is the optical router as it plays the major role in routing the packets in a network. The optical routers are fabricated from nanoscale photonic components which are very much susceptible to changes in temperatures and also susceptible inherent noises and crosstalk due to the physical structuring of the router. There are lots of proposed routers which have been introduced earlier in this dissertation each possessing distinct characteristics and performances. From the previous section of this dissertation we came across CRUX router which performs the best among all the proposed router and holds the place of being the most efficient router in terms of low noise generation and less crosstalk both at network level and router level. It supports passive routing and follows XY routing algorithm. At least one MR is turned on for every switching action except North-South, South-North, East-West, and West-East because of passive routing. CRUX takes the advantage of the PSE to minimize the losses and waveguide crossings. For example, Injection port uses PSE to reach West output and from North input to ejection port thereby reducing the number of waveguides and waveguide crossings. CRUX is the most compact 5x5 optical router. The dissertation also gives an insight to the thermal sensitivity of the photonic devices like VCSELs, optical waveguide, optical switches and optical receivers. We will get to know the effects of thermal-optic effect which hampers the performances of the optical networks as a whole and hence it gives us opportunity to research on the issue of thermal sensitivity and minimize it as much as possible. The next section will include some router modelling techniques and simulation of the router models and its evaluation.

5.1: Observations from Past Router Models.

A modelled router must be able to provide a high SNR, less crosstalk, and lower power consumption. Before diving into the process of designing optical router, it would be better to have a look at the previous proposed router such as Optimized Crossbar router, CYGNUS router and CRUX router with respect to the number of MR, number of crossings, number of optical terminators and the physical area etc. From figure 5, the Optimized Crossbar router contains 20 MRs, 10 terminators and 26 optical crossings, while from figure 4, the CYGNUS router contains 16 MRs, 2 terminators and 13 optical crossings. From figure 3, the CRUX router contains 12 MRs, 22 optical terminators and 9 optical crossing, one of the best performing optical routers with average loss of 0.64 dB followed by Cygnus router with average loss of 0.78 dB. Optimized crossbar has the highest average loss of 1.15dB which makes it the most power consuming optical router from among the optical routers.

The figure 3, 4 and 5 shows the three optical routers and by visualizing these routers structure, marked differences can be seen among these router structures. The Optimized Crossbar router has the highest average loss value because it contains the most number of crossings, optical terminators and MRs, also the area of the crossbar router is large when compared to CRUX router. The larger the area of an optical router the signal has to cover more distances which will lead to increase in propagation loss. The number of optical terminator used in an optical router also contributes the crosstalk noise in an optical router because in practical case the terminator are unable to absorb all the signal power because of the imperfect matched impedance creating power reflectance. The number of waveguide crossings also leads to increase in crosstalk noise because two signals of different wavelength intersects at a crossing and power of the two signal leaks to undesired output ports. The CRUX router average loss is significantly low because its design uses less number of optical resources and therefore the CRUX router design sets a benchmark for designing new router models. In order to design a router, there are few key points a designer must follow, such that the modelled router can perform better than the existing router.

1. Smaller area and shorter waveguides.
2. Less number of crossings.
3. Less number of terminators.
4. Less number of microresonators.
5. Passive routing paths.
6. Non-blocking.

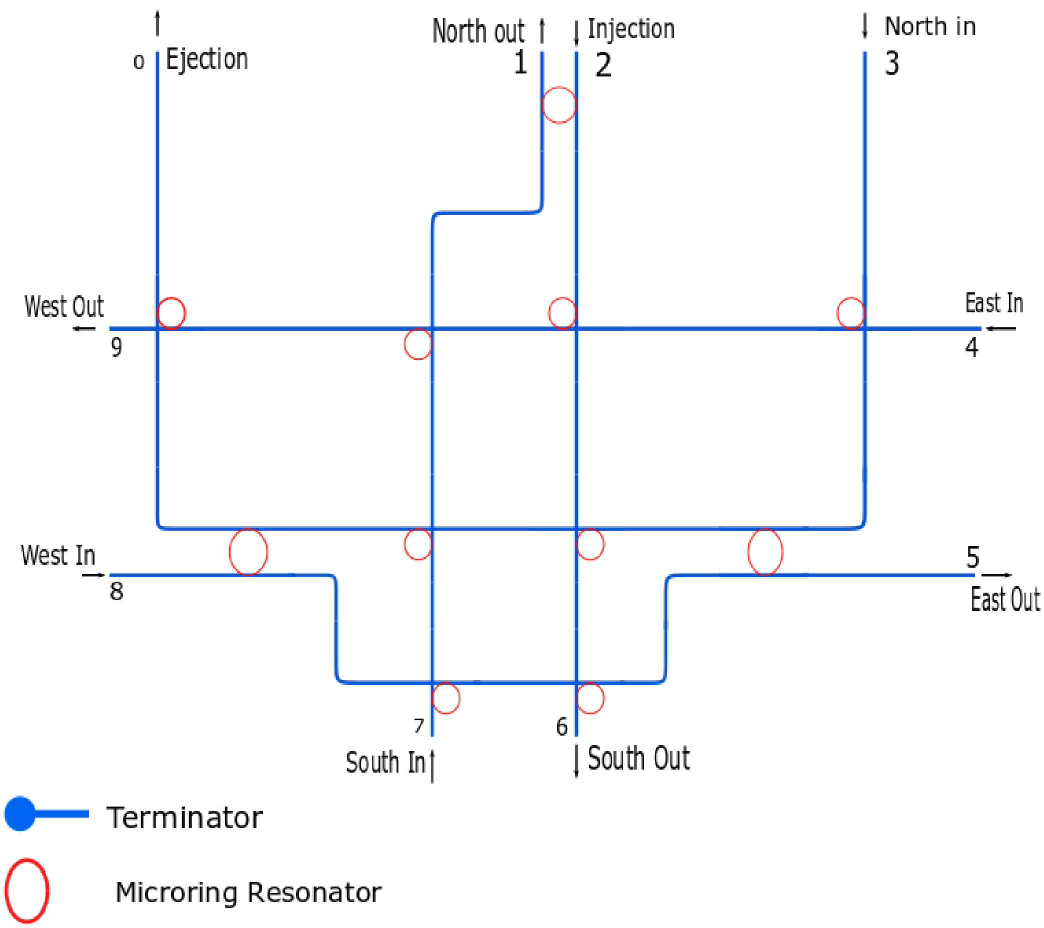

Figure 13: Modelled Router *RC1.3*

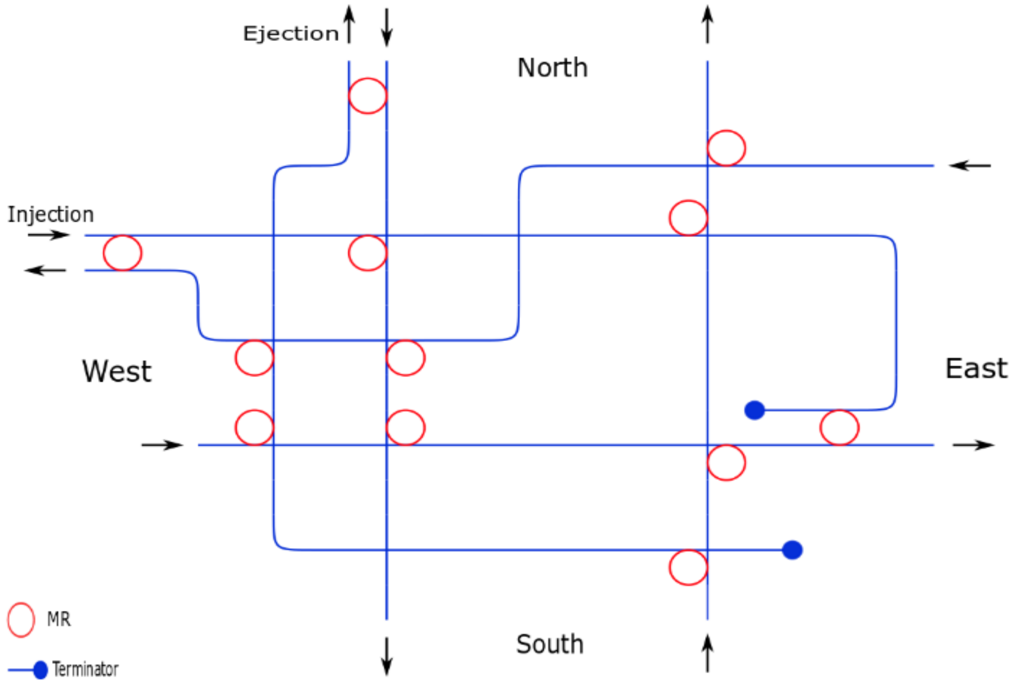

Figure 14: Modelled Optical Router *RC1.1*

5.2: Objectives behind modelling optical router.

There are lot of proposed optical routers with their own advantages and disadvantages over one another and still there lies plenty of room for improvement and an opportunity to produce more efficient optical routers which can be used in future ONoCs. This dissertation has provided information about some of the most recognised optical routers. In this dissertation, the primary objective is to model an optical router whose performance is better than today's state of the art optical routers. The objective will be achieved by simulating the designed router and comparing the observation results with existing optical router. The comparison will be made with the one of most efficient, CRUX, optical router. In order to model an optical router better than CRUX some steps must be followed, for example, the modelled optical router must contain less number of waveguide crossings, optical terminator, MRs and smaller area than CRUX. The figure 13 & 14 shows two of the modelled optical routers, *RC1.3* and *RC1.1*. The following section will provide information regarding structural aspect of the two modelled routers. The structural comparison between these routers will provide some information about the behaviour of the two routers during communication.

5.3: Modelled Routers.

Keeping in mind all the key points from the previous section about modelling an optical router. The figure 13 and figure 14 shows modelled optical routers named as *RC1.3* and *RC1.1* respectively, where *RC* stands for *Router Configuration*. The following points provides structural details about the two modelled routers referring from figure 13 and 14.

1. *RC1.1* contains a total of 12 switching elements, 9 CSE's and 3 PSE's. While, *RC1.3* contains a total of 11 switching elements, 8 CSE's and 3 PSE's. If compared with CRUX router, *RC1.3* has one less switching element which could help in reducing the crosstalk.
2. *RC1.1* contains 9 waveguide bendings and *RC1.3* contains 8 waveguide bendings thereby reducing the bending loss.
3. The number of physical waveguide crossings in *RC1.1* is 11, while in *RC1.3* the waveguide crossing is zero. The physical waveguide crossings are replaced by CSE's in *RC1.3.* A better performing router must contain less number of crossing to minimize the amount of crosstalk noise in a system, therefore *RC1.3* has greater chances of eliminating crosstalk noise than its modelled counterpart.
4. Both the modelled routers uses passive routing technique. In *RC1.1*, passive path exist between North-South, East-West and vice versa. But in case of *RC1.3* passive path exist between East-West, South-North, West-East and North-Ejection. There is no passive path between North-South ports which can lead to increase in power consumption because for every North- South signal transmission, additional power will be required for switching mechanism. These will led to more power consumption than RC1.1.
5. From figure 14, in *RC1.1*, there are three paths with long link lengths, these paths are South-Ejection, Injection-East, and East-West. These paths contains considerable amount for waveguide bendings and optical terminators which can lead to increase in power losses and crosstalk noise. For example, path Injection-East with 2 waveguide bendings, 2 waveguide crossings, 2 CSEs, a PSE and a terminator. While comparing with

RC1.3 in figure 13, there are two paths with long ling lengths. Out of the two longest links, path North-Ejection is the longest with 4 CSEs and two bendings. Although, this is a passive path but the signal has to travel long distance thereby will be consuming more power.

6. From the case study of existing optical router, it was seen that the number of optical terminator used in those designs lead to more crosstalks and power consumptions. Hence limiting the number of the optical terminators in a router design will be an important factor. The positive feature about *RC1.3* design is that it does not contain a single terminator which will help in reducing the reflected power and minimizing crosstalk noise.
7. To summarize, RC1.1 has a complex structure with more number of physical waveguide crossings, longer link length and there is no symmetry in the router design which is evident from the figure 14, which shows left side of the router design is congested with more optical components than right side creating an imbalance in power distribution during routing. While from figure 13, it could be seen that the *RC1.3* router design simple and the distribution of optical elements on both side of router design is even and therefore will lead to balanced power distribution pattern. From the observations, it can be predicted that the *RC1.3* will perform better in minimizing crosstalk noise and will have a better SNR when compared to *RC1.1*. The next chapter is based on simulations and observation which will reveal the best optical router between the two modelled routers.

………………

Chapter 6.

Comparison of the optical routers.

The primary aim in this work was to design optical routers performing better than the other existing optical routers. Simulations result will prove that the designed routers are working properly and performing as per requirements. The CLAP simulation tool helped to simulate the modelled router for signal power, crosstalk noise and SNR. The designed routers were simulated for single wavelength mode as well as WDM mode. The simulations were performed on a router level and also on a network level. Network level simulations were carried out in 8x8 Mesh based network topology. For each signal performance parameters, more than 100 simulations where performed and the observations were recorded. The recorded data from the simulations were used for comparison with the existing data of the CRUX router. CRUX optical router was used as a reference because it is the most efficient optical router. The primary objective of the work could be achieved only when an improvement in performances of the modelled routers from the previous routers are identified during evaluation of the simulation results. This section compares two of the modelled routers with CRUX router in router level as well as in network level simulations. In router level, the routers were compared on the basis of number of elements, power at output ports and power at the input ports. While in network level, these routers are placed in the 8X8 mesh based network topology.

6.1: Comparison between Modelled Routers on Router level

Simulation on a router level was the first task after designing the routers because the router level simulation brings up fault in the modelled design. The router level simulation helped in finding the powers received at the output port for a given input power and the amount of crosstalk noise present across other ports. During simulation, all the input ports were provided with 1mw of power. The table 4 and table 5 will provide a comparison between two modelled routers, the *RC1.1* and *RC 1.3* on the basis of the number of optical components used for a particular input and output link.

port in	port out	#waveguides	#CSE	#PSE	# physical crossing	#waveguide bends	#total elements
North	Ejection	7	4	2	0	2	15
North	East	3	1	1	0	1	6
North	South	4	3	1	0	1	9
North	West	4	4	0	0	0	8
East	North	2	2	1	0	0	5
East	South	3	4	0	0	0	7
East	Ejection	4	4	0	0	0	8
East	West	3	4	0	0	0	7
South	North	2	3	1	0	0	6
South	East	2	2	1	0	2	7
South	West	3	4	0	0	0	7
South	Ejection	3	3	1	0	1	8
West	Ejection	3	1	1	0	1	6
West	South	2	2	1	0	2	7
West	North	3	3	2	0	4	12
West	East	3	2	2	0	4	11
Injection	North	0	0	1	0	0	1
Injection	South	3	3	1	0	0	7
Injection	East	4	3	2	0	2	11
Injection	West	3	3	1	0	0	7

Table 4: Count of Optical Element in RC1.3

port in	port out	#waveguides	#CSE	#PSE	# physical crossing	#waveguide bends	#total elements
North	Ejection	0	0	1	0	0	1
North	East	6	4	2	0	0	12
North	South	4	3	1	1	0	9
North	West	3	3	2	0	2	10
East	North	2	1	0	0	0	3
East	South	6	3	0	2	0	11
East	Ejection	6	3	1	1	2	13
East	West	5	3	1	1	4	14
South	North	3	4	0	0	0	7
South	East	3	2	1	0	0	6
South	West	6	6	1	1	4	18
South	Ejection	5	3	1	2	3	14
West	Ejection	2	2	1	1	2	8
West	South	2	2	0	1	0	5
West	North	4	5	0	0	0	9
West	East	4	3	1	0	0	8
Injection	North	5	3	1	2	0	11
Injection	South	5	3	1	2	0	11
Injection	East	7	2	2	2	2	15
Injection	West	1	0	0	0	0	1

Table 5: Count of Optical Elements for Router RC1.1

The table 4 and 5 provides the data regarding the total number of optical elements used on a communication path for particular input/output port combination. The tables shows total number of CSE's, PSE's, physical crossings, and waveguides for both the modelled routers. An interesting fact, the CSE's involves crossing which accounts for crosstalk noise, therefore number of CSE's in a signal propagation path directly contributes to crosstalk noise. The physical waveguide crossings in *RC1.3* is absent, therefore the crosstalk noise generated in *RC1.3* will be due to CSE's along the signal path. While *RC1.1* contains 3 physical waveguide crossings and 12 CSE's therefore the total number of crossing inside *RC1.1* is 15, thereby it could be expected that *RC1.1* will be prone to more crosstalk noise than *RC1.3*. Number of optical elements plays a very important role in an optical link because the optical elements are susceptible to temperature changes and different kinds of losses are associated with them. Each element has its own loss coefficient, as shown in table 3, hence different element affects the signal differently while passing through them. Comparing two of the modelled routers, *RC1.1* and *RC1.3,* by looking at the total number of elements column in table 4 and table 5, it can be seen that the router *RC1.1* has higher number of elements for most number of the paths than *RC1.3*. For example, the highest number of elements for *RC1.1* for South-West link, is 18 while for *RC1.3* is 7 for that particular link, therefore it can be predicted that for network level simulation, if this particular path is used too often, networks with router *RC1.1* will suffer more signal degradation and power losses than network with router *RC1.3*. Knowing the number of elements in an optical path at the router level helps in calculating, the total number of optical elements at network level, hence enabling the designer to analyze the losses on a network level and make necessary changes in the router design, for example, the modelling of *RC1.1* was designed prior to the modelling of *RC1.*3 and hence the router design *RC1.3* is an improved version with much lesser optical elements. The router level simulation also provides the power consumption of an individual router for each input-output combination. A comparison between two routers has been shown graphically which will lead to some interesting findings and can be used to predict the results in network level.

Input-output	RC1.1 in (mw)	Rc1.1 out (mw)	RC1.3 in (mw)	RC1.3 out (mw)
North-Ejection	1	0.926608	3.50973	0.72744
North-East	3.35457	0.715359	1.8664	0.874891
North-South	4.04739	0.801072	2.38011	0.790295
North-West	3.40258	0.740493	2.87023	0.783796
East-North	1	0.926531	4.65538	0.77506
East-South	4.16002	0.811936	3.14696	1.53879
East-Ejection	5.03	0.759108	3.52468	0.783796
East-West	4.38303	0.797038	4.05163	0.800412
South-North	4.24607	0.801117	4.6056	0.806317
South-East	1.91191	0.837131	1.81586	0.834712
South-West	5.88439	0.648944	3.2076	0.784108
South-Ejection	4.05813	0.774403	2.50476	0.790295
West-Ejection	2.55168	0.827379	1.7634	0.874891
West-South	2.65231	1.70491	1.85224	1.63824
West-North	4.86315	0.72855	3.97423	0.738164
West-East	3.60776	0.80847	2.57705	0.743685
Injection-North	4.20342	0.777286	1	0.926608
Injection-South	3.92283	0.777352	3.07435	0.808034
Injection- East	4.24524	0.775171	2.50941	0.75368
Injection-West	1	0.926608	2.22958	0.79135

Table 6: Input and output powers at different ports of RC1.1 and RC1.3

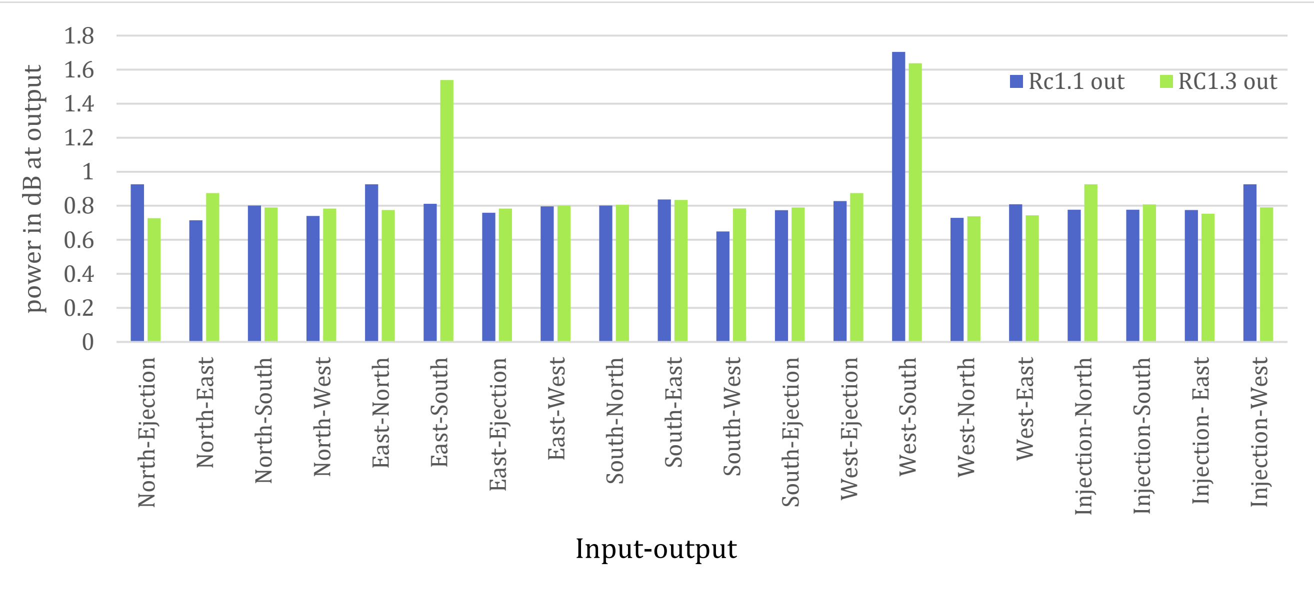

Figure 15: Histogram view of output powers

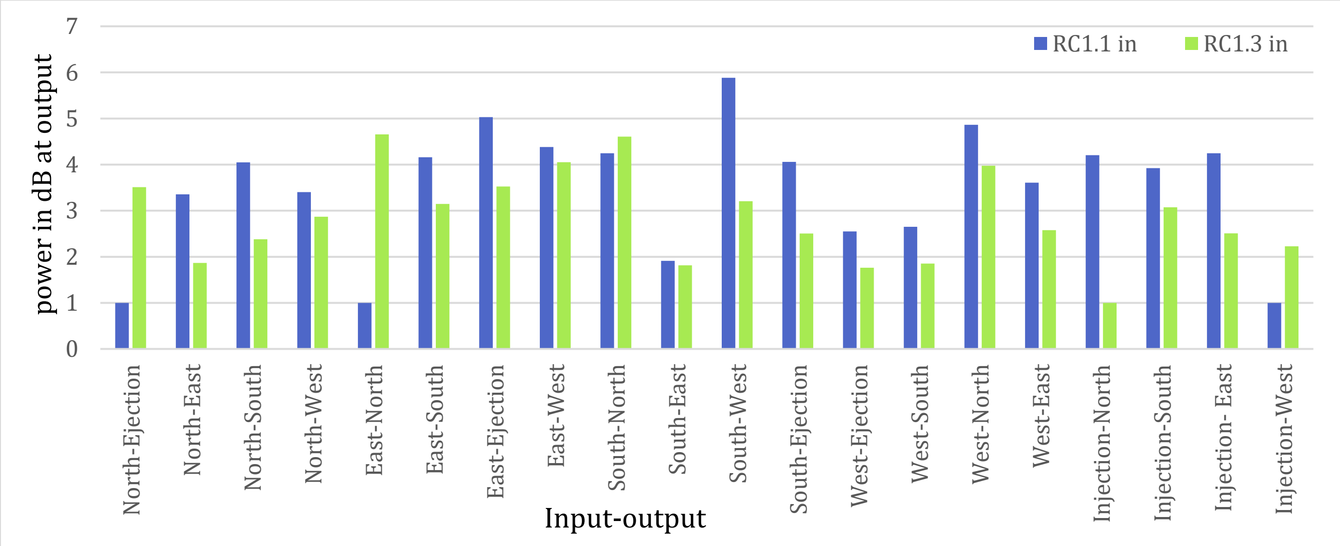

Figure 16: Histogram view of input powers

The table 6 and its graphical representation of the power obtained at the output ports and input ports for each input-output combination has been shown in figure 15 and figure 16, respectively. Some observations which has been listed out from the above tables:

1. It can be seen that with an equal number of elements in different communication link, the output powers of the each link are different because each element in a link contributes to losses in different amounts, for example, an optical waveguide's contribution to losses is proportional to its length. For example, in table 4 and table 5, two communication node with same number of element for both modelled router i.e. South-North path for *RC1.1* and South-East for *RC1.3*, each path contains total of 7 elements, while the South-North Communication link has less output power when compared to South-East link because the South-North link contains 2 extra CSE when compared to South-East link referring from output power values shown in Table 6. Therefore, it can be said that CSE's contributes to more power losses.
2. For a North-South communication path, *RC1.1* output power is better than *RC1.3* even if there are the same number of elements because *RC1.3* contains a waveguide bending which can lead to extra bending losses and signal scattering.
3. The table 6 also provides an interesting findings that for different links if the total number of optical elements containing the exact same type of elements, the output power will be exactly same, for example, two links, North-East and West-Ejection, for

RC1.3 have the same output power, which hints at the fact that the link lengths are equal for the router design. Another example can be seen in *RC1.1* for two different links, Injection-North and Injection-South the output power are same. So from this observation it can be pointed out that if the number of elements and the link length are same the power loss will be same.

4. The second graphical representation in figure 16 provides signal power received at the input port. As the input power for all the input ports are 1 mw but the power shown in table 6 for input ports is more than 1 mw, this points out the fact that the extra power recorded at the input ports are additional power require to compensate for the losses in signal propagation. A router can be treated as a better performing router when the additional power received at the input power is minimum. Comparing *RC1.1* and *RC1.3* in terms of power at the input port it can be seen from figure 16 that the power at input port for *RC1.3* is lower than *RC1.1* which hints towards the fact the crosstalk noise in *RC1.3* will be less compared to *RC1.1*.
5. The extra power at the input port can be due to complexity of the router design for example, a complex router will have more waveguide crossings, CSEs, waveguide bendings etc. In a complex design, the distribution of the optical elements across the overall router area might not be balanced as seen from router design *RC1.1* in figure 14, which shows more congestion in left side of the network and can generate more noise power leading to increase in power at the input port. This observation is clearly seen in table 6, where the input port power of router *RC1.1* is significantly higher than *RC1.3*, which has a balanced element distribution.
6. From the router level simulations and evaluations, some conclusion can be drawn about designing an optical router. The router design should be simple and there must even distribution of elements and avoiding congestions. Minimizing the number of elements used in a communication link inside a router to less than 8. Form the table 6, it could be concluded that in *RC1.3* has less crosstalk noise than *RC1.1* hence in the next section a comparison between *RC1.3* and CRUX has been carried out.

Input-output	CRUX in (mw)	CRUX out (mw)	RC 1.3 in(mw)	RC1.3 out(mw)
North-Ejection	1	0.926608	3.50973	0.72744
North-East	1	0.657982	1.8664	0.874891
North-South	1	0.82928	2.38011	0.790295
North-West	1	0.805678	2.87023	0.783796
East-North	1	0.925586	4.65538	0.77506
East-South	4.02727	0.739781	3.14696	1.53879
East-Ejection	1.91191	0.828071	3.52468	0.783796
East-West	3.45876	0.808631	4.05163	0.800412
South-North	3.45278	0.805747	4.6056	0.806317
South-East	1.9117	0.829351	1.81586	0.834712
South-West	4.49221	0.662864	3.2076	0.784108
South-Ejection	3.31469	0.764808	2.50476	0.790295
West-Ejection	4.0024	0.734374	1.7634	0.874891
West-South	3.341996	0.772301	1.85224	1.63824
West-North	3.44201	0.80272	3.97423	0.738164
West-East	1	0.9255	2.57705	0.743685
Injection-North	1.77717	0.833104	1	0.926608
Injection-South	3.31719	0.778032	3.07435	0.808034
Injection- East	3.36095	0.772212	2.50941	0.75368
Injection-West	1	0.926608	2.22958	0.79135

Table 7: Input and output powers at different ports of CRUX and RC1.3

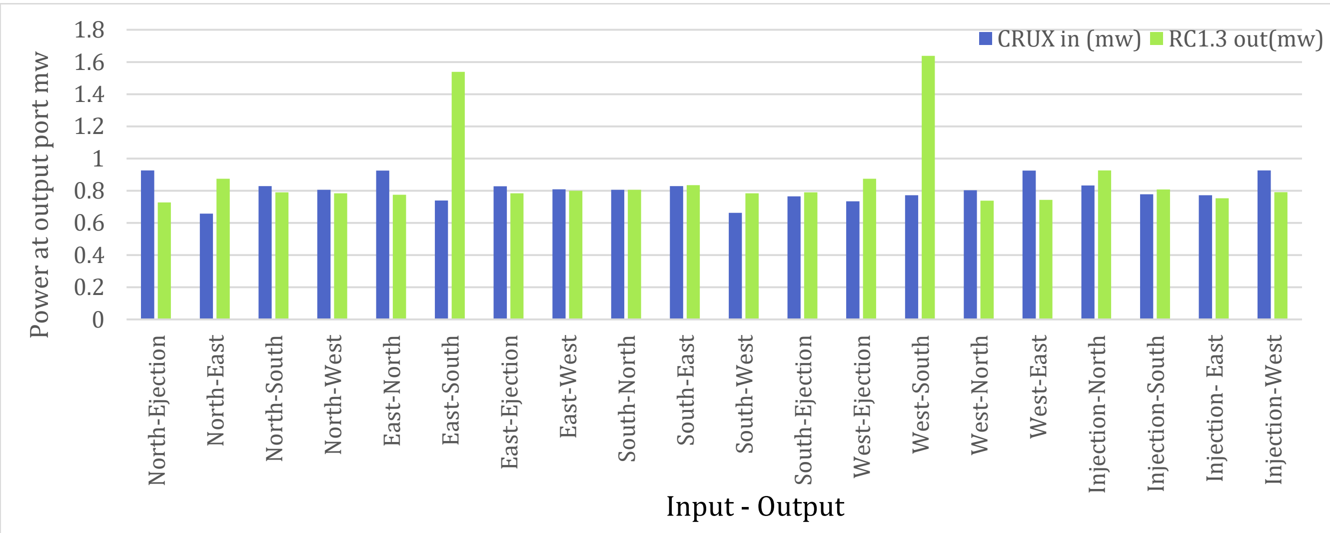

Figure 17: Graphical View of comparison between CRUX and RC1.3 for Output port power.

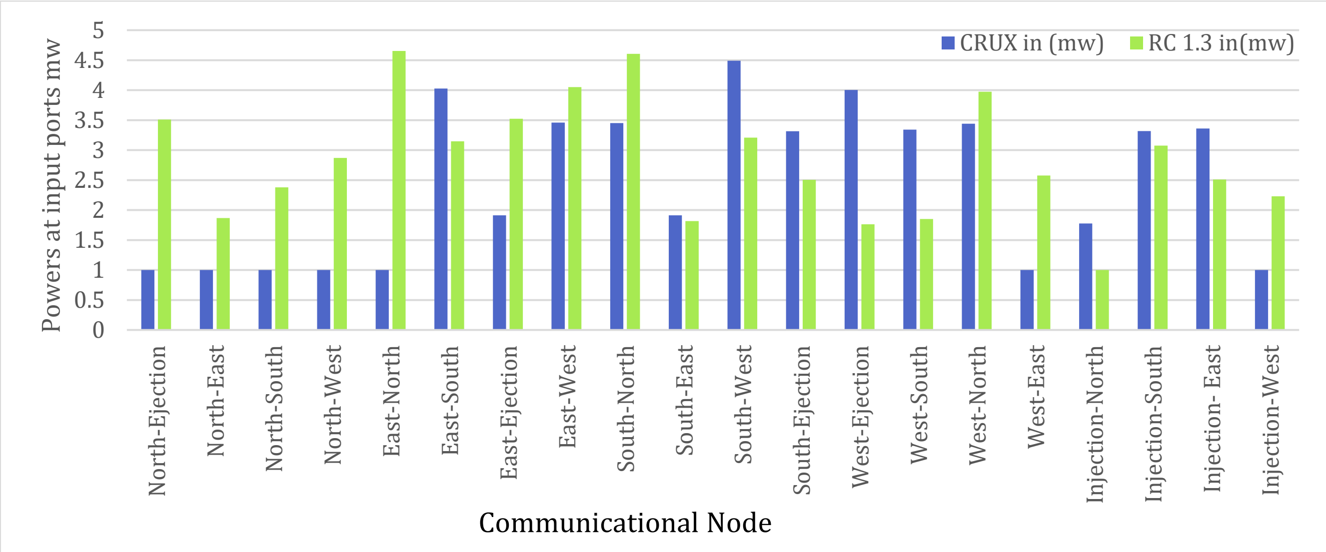

Figure 18: Graphical View of comparison between CRUX and RC1.3 for power at input port.

6.2: Comparison between CRUX and RC1.3 in Router Level.

After the evaluation of both modelled router it can be concluded that the performance of *RC1.3* is better than *RC1.1* from router level comparison on input power and output power at different ports, therefore a comparison between CRUX and *RC1.3* is necessary to find out whether *RC1.3* performance is superior to CRUX at router level. The analysis will be conducted on the basis of the table 7 and the graphical representation in figure 17 and figure 18. The Observations were as follows.

1. There are 10 communicational links where the total number of elements in a communication link for *RC1.3* is less than CRUX. For those particular links, the power in the output port is higher than CRUX.
2. The average output power for 1 mw input power for CRUX is 0.806402 mw while that of *RC1.3* is 0.881619 mw.
3. Noise power at input ports of *RC1.3* is considerably higher than the CRUX router.
4. CRUX has no noise power for the North input port which is not the case with *RC1.3*.
5. It can be seen that almost every input port of *RC1.3* needs extra power, highest being east input port i.e. 4.65538 mw.

After analysing, the above tables which shows the powers at the different output ports and input ports, it can be concluded that between the modelled routers, *RC1.1* and *RC1.3*, the better performing router is *RC 1.3* because the design is simple and it contains less number of crossings and showing symmetric architecture. The simple design makes it less prone to crosstalk noises and signal losses, almost 70-80 percent of the input power reaches the output ports. *RC1.3* has less number of MR and zero waveguide crossings and terminators hence the amount of crosstalk and backward reflection is lower in the router. While comparing *RC1.3* from CRUX on router level, it can be evaluated that the input noise power for *RC1.3* is significantly higher than CRUX, this behaviour is possible due to waveguide bendings present in the design leading to increase in input power. The important and positive outcome of *RC1.3* is that its average output power is more than the CRUX.

6.3: Comparison between Modelled Routers on network level.

The modelled routers were placed in 8x8 mesh-based network topology and simulations were carried out for signal power, coherent crosstalks and SNR. The simulation values for SNR, signal power and coherent crosstalk for different communicational nodes provided necessary data which helped in performance evaluation of three different routers - CRUX, RC1.1 and RC1.3. In the following section detailed analysis will be provided based on the observations of the simulations process and a short hypothesis will be followed which will points out the factors for selecting a better router among the modelled router.

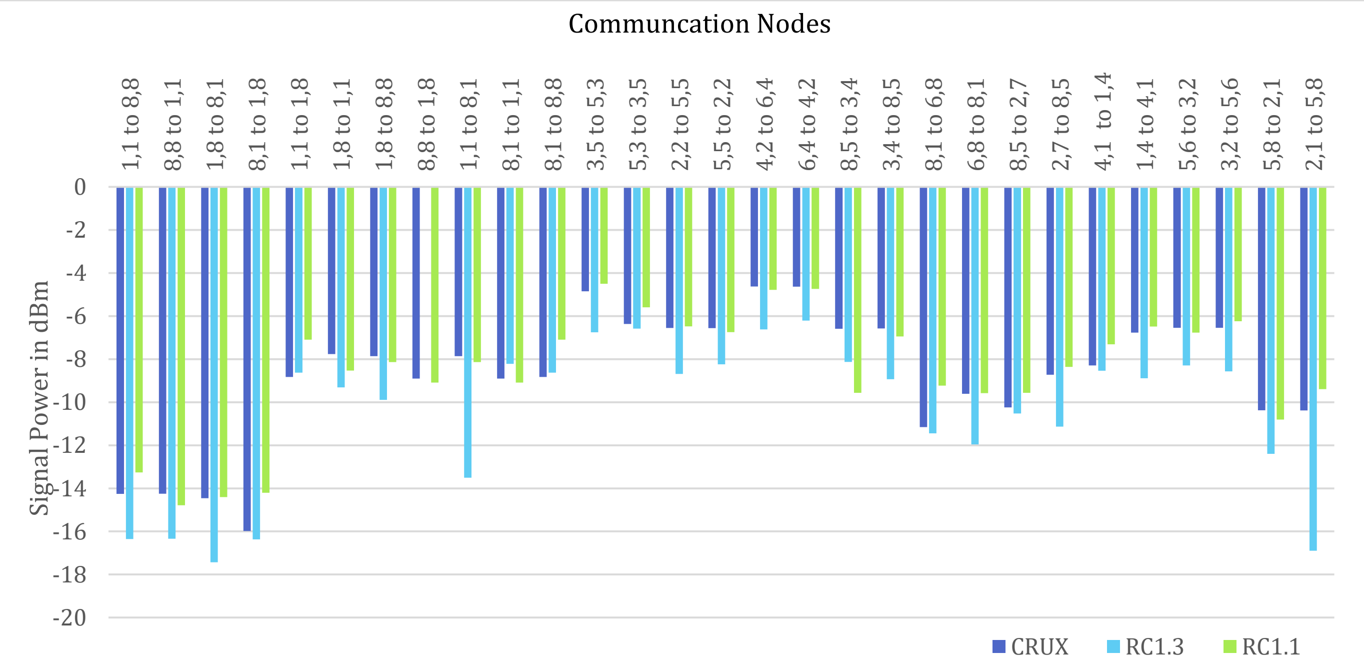

Figure 19: Router comparison on the basis of signal power.

Communication Path	CRUX Signal Power	RC1.3 Signal Power	RC1.1 Signal Power
1,1 to 8,8	-14.2594	-16.3564	-13.2562
8,8 to 1,1	-14.2461	-16.3403	-14.7832
1,8 to 8,1	-14.4572	-17.4307	-14.4079
8,1 to 1,8	-15.9832	-16.3719	-14.2012
1,1 to 1,8	-8.8267	-8.62376	-7.09652
1,8 to 1,1	-7.76242	-9.30814	-8.52846
1,8 to 8,8	-7.8591	-9.88973	-8.13851
8,8 to 1,8	-8.90434	-8.21426`	-9.08751
1,1 to 8,1	-7.8591	-13.5066	-8.13851
8,1 to 1,1	-8.90434	-8.21426	-9.08751
8,1 to 8,8	-8.8267	-8.62376	-7.09652
3,5 to 5,3	-4.84405	-6.75465	-4.49902
5,3 to 3,5	-6.36646	-6.58072	-5.58745
2,2 to 5,5	-6.55205	-8.68718	-6.47446
5,5 to 2,2	-6.55708	-8.23709	-6.74315
4,2 to 6,4	-4.62522	-6.61953	-4.77993
6,4 to 4,2	-4.63482	-6.21129	-4.73315
8,5 to 3,4	-6.58812	-8.12877	-9.5631
3,4 to 8,5	-6.57543	-8.93279	-6.94817
8,1 to 6,8	-11.1543	-11.4428	-9.23165
6,8 to 8,1	-9.6109	-11.9545	-9.57945
8,5 to 2,7	-10.242	-10.524	-9.5631
2,7 to 8,5	-8.72109	-11.1355	-8.36178
4,1 to 1,4	-8.29292	-8.53896	-7.3102
1,4 to 4,1	-6.76668	-8.88985	-6.4808
5,6 to 3,2	-6.54156	-8.29124	-6.76533
3,2 to 5,6	-6.54036	-8.56437	-6.23761
5,8 to 2,1	-10.3706	-12.397	-10.8075
2,1 to 5,8	-10.3823	-16.9006	-9.38982

Table 8: Router comparison on the basis of signal power for different communicational nodes

Simulation process was carried out three times, starting from CRUX followed by *RC1.1* and finally with *RC1.3*. The communicational nodes were predefined in the input.txt file of the CLAP simulation tool. The communication nodes in the tables includes communication nodes with maximum distance-path as well as minimum distance-path across the mesh-based network. The maximum distance-path was the path with most number of routers in communicating path, example from node (1, 1) to node (8, 8) or vice-versa and the smallest distance-path was the communication path between adjacent nodes. The CLAP simulations on network level provided results for the signal power, coherent and in-coherent crosstalk and SNR for single wavelength and also for multiple wavelength. The routing of the signal around the network is based on XY routing topology. The simulations were performed for approximately 100 communicational path but all the results is impossible to be presented here, however, a sample set of the simulation results has been shown and comparison has been done on the basis of the provided sample set.

a. Comparison on basis of Signal powers

Signal power plays a vital role for a successful communication across a network. Signal power in a network-on-chip is an expensive resource which must be utilized very carefully because the signal power is directly proportional with the power consumption inside a network. A badly designed router will consume more power than an efficient router. The signal power compensates for the losses accompanied in the network for badly designed routers.

In this section, the routers has been compared on the basis of signal power on network level. The signal power unit is in logarithmic scale (dBm). During the simulation, the signal power was measured for a given communication link between two nodes of 8x8 mesh-based network topology. The observation values between the three routers has been shown both on tabular in table 8 and graphical form in figure 19. Some observations of the simulation are:

1. The received signal power tends to decrease if the number of crossing, bending and signal droppings from a CSE increases along communication paths leading to signal dispersion and interferences thereby creating reduction in signal power at receiving side. The increased reduction in signal power has been shown by the increase in negative logarithmic values in figure 19.

1. 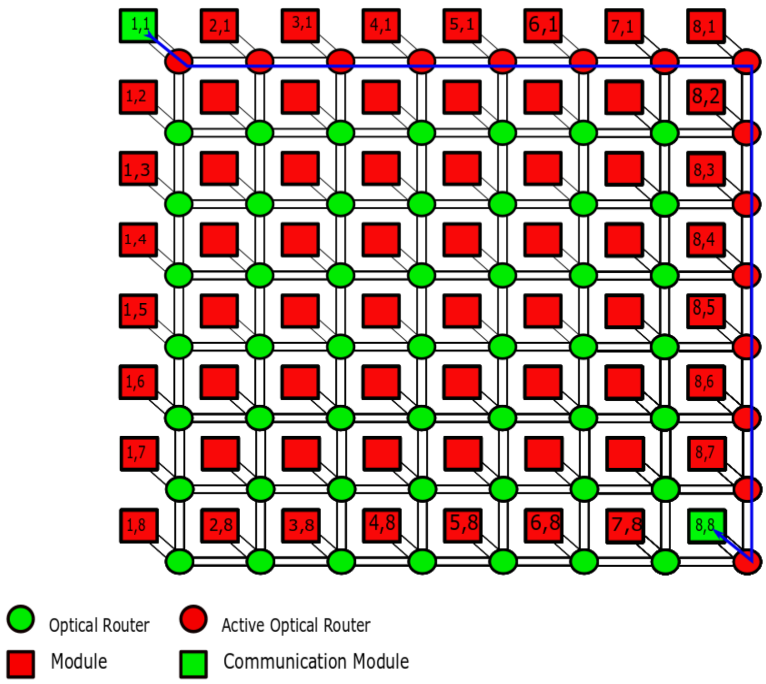

Figure 20: Communication between modules (1, 1) and (8, 8) in an 8x8 Mesh Topology.

2. The graphical representation in figure 19 depicts that the minimum and maximum signal recorded for CRUX Router is -15.9832 dBm and -4.62522 dBm, respectively. On the contrary, the *RC1.3* is able to achieve a minimum and maximum signal power of -17.4307 dBm and -6.21129 dBm respectively while *RC1.1* has signal power of -14.7832 dBm and -4.49902 dBm.
3. The signal power consumption is directly related to the number of optical elements along the links and the link length. For example, consider communication node (3, 5) to (5, 3), the total number elements along this particular link is 45 for *RC1.3,* 30 for *RC1.1* and 21 for CRUX, it can be approximated that for this particular communication CRUX's signal power will be better than the other two but it can be seen that signal power for *RC1.1* is better than others which can be due to the fact that the link length of *RC1.1* is less when compared with *RC1.3* and CRUX.
4. It could be said that the longest communication link is not always the link with the most degraded power. For example, the longest link in an 8x8 mesh-based network is (1, 1) to (8, 8) and vice versa, must be the path where the signal power values must be the lowest but results shows otherwise. Therefore from this observation, it can be concluded that the longest links in a network are not always prone to higher losses.

5. It has been observed that the signal power for all the three routers for bidirectional communication is almost similar although the path taken is totally different. For example, figure 20 shows communication between modules positioned at point (1, 1) and (8, 8), the path followed is marked by a blue line. The reverse communication path between nodes (8, 8) to (1, 1) can be figured out using XY routing topology but the signal power remains almost approximately similar. This observation could only take place when the router design is symmetrical and distribution of optical elements along both the communication links is similar.
6. On the basis of signal power values, *RC1.1* has better signal power values for the given communicational links. Signal power consumption of *RC1.1* comparatively less than *RC1.3* because *RC1.1* fully utilizes the passive routing technique, for example in *RC1.1* the East-West, West-East, North-South and South-North communication is do not require any switching while in *RC1.3* North-South path switching requires a CSE, hence for any communication link where signal must travel North-South direction through a *RC1.3* router requires an additional CSE for switching, this will lead to increase in signal power consumption.
7. Comparing *RC1.1* and CRUX router, the signal power of *RC1.1* is approximately similar to CRUX router for most of the observations but there are cases where *RC1.1* performs better than CRUX, for example, node (1,1) –(8,8) ,(8,1)-(1,8) ,(8,1)- (6,8), (4,1)-(1,4) etc. This is due to the fact that *RC1.1* contains less crossings, bendings and the overall link length is lesser than CRUX router.
8. From the above observation, it can be concluded that proper utilization of a passive routing technique is a necessity while designing an optical router because this technique considerably brings down the numbers of switching mechanism along a communicating link resulting in lowering of power consumption. Passive routing also helps in keeping the maximum number of switching taking place in signal routing to 3. The increase in link length inside a router creates an overall increase in length between two nodes and thereby creating an increase in propagation loss. Example, the figure

13 shows the model of *RC1.3* where it can be seen that the signal coming from North input port has to travel a long path before reaching the Ejection port, while in figure 14, the *RC1.1* model, the signal is switched from North input to Ejection port via a PSE and the distance travel by the signal is way more less than the distance travelled by signal in *RC1.3*. Therefore, the distance travelled by a signal inside a router is also a very important parameter which could be controlled by proper designing technique.

b. Comparison on the basis of coherent crosstalk.

Crosstalks are unwanted interfering signals from various sources in a system. The crosstalk can be caused due to signal leakage at a waveguide intersection, reflection from an optical terminator, leakage from a microring resonator. Crosstalk noise is unavoidable in a real world scenario but could be minimized by proper control mechanisms. In a communicational network crosstalk noise can produce erroneous signal reception, loss of data packets, lowering of SNR etc. The crosstalk noise across a network must be kept to a minimum in order to provide maximum throughput. The major portion of crosstalk noise in optical networks comes from optical routers. The reduction of crosstalk at router level can result in overall reduction of crosstalk noise. The CRUX router is the most efficient optical router with high SNR and low crosstalk noise. In this section, the modelled optical router, *RC1.1* and *RC1.6* will be simulated using the CLAP tool where the communication nodes are provided as the input to the CLAP and the result for crosstalk noise are recorded for each communicational node.

The crosstalk noise values are in logarithmic scale (dBm), the crosstalk noise values must be in negative decibels which marks for lower crosstalk noise along the link. The table 9 and figure 21, shows a comparison between the three routers on the basis of coherent crosstalk noise for different communication nodes in an 8x8 mesh based network.

Communication Nodes	CRUX Coherent Crosstalk dBm	RC1.1 Coherent Crosstalk dBm	RC1.3 Coherent Crosstalk dBm
1,1 to 8,8	-32.2439	-31.295	-41.0941
8,8 to 1,1	-32.2306	-32.7677	-40.246
1,8 to 8,1	-32.4226	-32.4116	-41.567
8,1 to 1,8	-39.8147	-38.5656	-40.1304
1,1 to 1,8	-18.3646	-25.6317	-35.3926
1,8 to 1,1	-26.2543	-1.78329	-35.9345
1,8 to 8,8	-35.0699	-35.1914	-36.8058
8,8 to 1,8	-35.5152	-35.6983	-35.2827
1,1 to 8,1	-26.351	-26.6089	-31.9556
8,1 to 1,1	-27.3109	-27.4941	-35.2827
8,1 to 8,8	-35.4375	-34.6416	-35.3926
3,5 to 5,3	-23.6483	-23.3497	-35.2843
5,3 to 3,5	-25.034	-24.3001	-35.1104
2,2 to 5,5	-25.1973	-25.0974	-35.9135
5,5 to 2,2	-25.2023	-25.3884	-35.6274
4,2 to 6,4	-23.4526	-23.5611	-35.1492
6,4 to 4,2	-35.3674	-35.4658	-35.1986
8,5 to 3,4	-25.2333	-25.344	-35.519
3,4 to 8,5	-25.2207	-25.527	-36.4934
8,1 to 6,8	-36.7681	-35.7046	-36.9622
6,8 to 8,1	-35.9502	-36.1903	-37.4739
8,5 to 2,7	-36.3258	-35.9024	-36.501
2,7 to 8,5	-27.1701	-35.5726	-37.624
4,1 to 1,4	-26.7848	-25.8671	-35.6074
1,4 to 4,1	-25.3897	-25.1484	-36.1162
5,6 to 3,2	-25.1868	-25.4106	-35.6815
3,2 to 5,6	-25.1856	-24.8828	-35.6328
5,8 to 2,1	-28.6729	-29.1098	-37.7045
2,1 to 5,8	-28.6846	-27.7544	-27.488

Table 9: Router comparison on the basis of coherent crosstalk for different communicational nodes

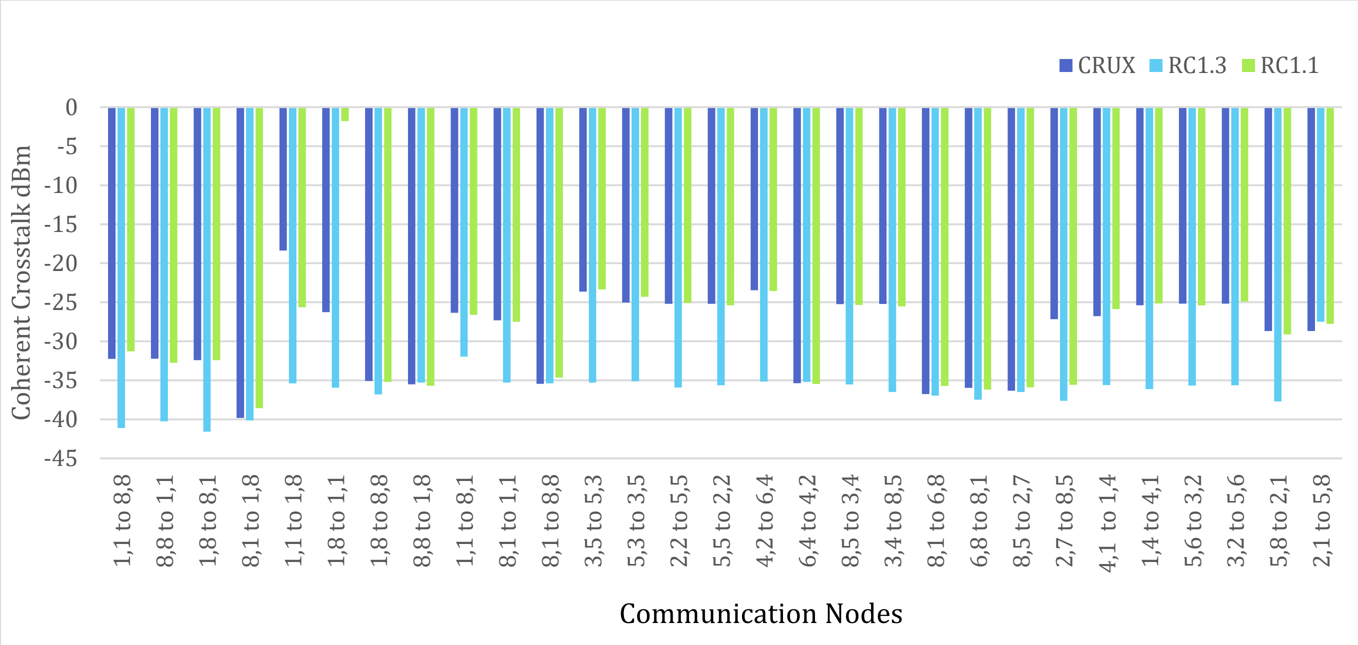

Figure 21: Router comparison on the basis of coherent crosstalk.

From the graphical representation of the table 9, the observation are as follows:

1. The minimum value crosstalk noise for CRUX, *RC1.1* and *RC1.3* are -18.3646 dBm, -1.78329 dBm, -27.488 dBm respectively and the maximum crosstalk values are -39.8147 dBm, -41.567 dBm and -38.5656 dBm respectively.
2. From the table 9, the third column represents crosstalk values of *RC1.3*, it could be seen than the longest link has the minimum crosstalk value, i.e. -41.567 dBm, which reflects the capability of *RC1.3* router to lower down the crosstalk noise at router level. The crosstalk values obtained after the simulation were very interesting because the crosstalk values for the most of given communication link samples were lower than -35 dBm showing that *RC1.3* router was less susceptible to crosstalk noises.
3. On comparing the crosstalk values of *RC1.3* with other two routers for all communicational nodes, it is observed that the *RC1.3* crosstalk values were lower than the other two routers in comparison. Average value of coherent crosstalk being -36.2068 dBm which enabled the router to perform efficiently and effectively during the high traffic conditions across the network.
4. The crosstalk noise values of *RC1.1* is more than CRUX optical router because at router level *RC1.1* router design contains more number of crossings and two optical terminator and nine waveguide bendings which enhances the crosstalk noise power,

while CRUX router has 9 waveguide crossing and one optical terminator hence the crosstalk values are lower. In the router design of *RC1.1* in figure 14, it could be seen that there are three paths inside the router where signal has to travel long links for example East-West, South-Ejection and Injection-East, with terminators place at South-Ejection and Injection-East path contributing to more crosstalk noises. The CRUX, on the other hand has shorter link lengths making it less susceptible to crosstalk noise.

5. The lower values of crosstalk in *RC1.3* were due to the fact that router design contains less number of CSE, no optical terminators, and no waveguide crossings. In fact if *RC1.3* is compared with CRUX router design the number of crossing in CRUX is 9 while in RC1.3 is 8, one optical terminator is used in CRUX while none in RC1.3. The physical waveguide crossing is not available in *RC1.3* because it has been replaced by CSE crossing contributing more towards lowering of crosstalk noise.
6. From the table 9, it could be seen that for a longest link length, for example from (1,1) to (8,8), the crosstalk noise values for RC1.3 is -41.0941 dBm which is 10 dBm lower than the other two routers in comparison. For each and every communication node the crosstalk noise for RC1.3 is 5 to 10 dBm lower than other routers in comparison. The results show that RC1.3 has good capability of lowering down the crosstalk noise and could be superior to CRUX optical router when it comes to crosstalk noise reduction.

b. Comparison Based on Signal to Noise Ratio (SNR).

The SNR is one of the most important parameters when it comes to communication scenarios. The SNR provides the information about the overall noise present in a system, it is also desirable that the SNR should be as high as possible for a clear and unaltered reception of data launched by the transmitting side The SNR value must be always positive for a better reception of the data at the receiving end while negative SNR indicates presence of high noise power in the transmitting signal. The CLAP tool will provide SNR results for three routers in comparison and the unit will be in dB.

Communication Path	SNR CRUX dB	SNR RC1.3 dB	SNR RC1.1 dB
1,1 to 8,8	23.8641	23.0521	19.5263
8,8 to 1,1	23.3547	22.8293	23.3896
1,8 to 8,1	20.7631	19.9063	17.0643
8,1 to 1,8	23.8315	23.7585	24.38
1,1 to 1,8	19.4314	16.9282	15.7702
1,8 to 1,1	16.424	17.5419	14.5139
1,8 to 8,8	27.2264	26.916	27.0684
8,8 to 1,8	26.6264	27.0684	26.6264
1,1 to 8,1	26.3555	25.4577	1.69396
8,1 to 1,1	23.8315	22.8293	23.3896
8,1 to 8,8	26.6264	26.7688	27.5606
3,5 to 5,3	14.2693	6.32011	-6.28431
5,3 to 3,5	9.22045	3.81061	8.6332
2,2 to 5,5	17.8359	12.815	4.15604
5,5 to 2,2	6.99089	10.3204	7.33436
4,2 to 6,4	1.1096	1.37418	-4.81034
6,4 to 4,2	30.7482	26.8156	30.7482
8,5 to 3,4	2.28804	6.50901	7.5471
3,4 to 8,5	20.1597	18.8371	8.80897
8,1 to 6,8	25.6294	25.5194	26.4885
6,8 to 8,1	26.3549	25.339	26.6264
8,5 to 2,7	26.0993	25.977	26.3549
2,7 to 8,5	21.329	16.0311	27.2264
4,1 to 1,4	0.125423	-1.39947	3.93923
1,4 to 4,1	18.083	15.8399	15.3607
5,6 to 3,2	2.37088	1.55739	4.19408
3,2 to 5,6	-3.30289	0.974483	0.785295
5,8 to 2,1	5.15477	3.57835	7.99297
2,1 to 5,8	0.918779	14.9111	5.11343

Table 10: Router comparison on the basis of SNR for different communicational nodes

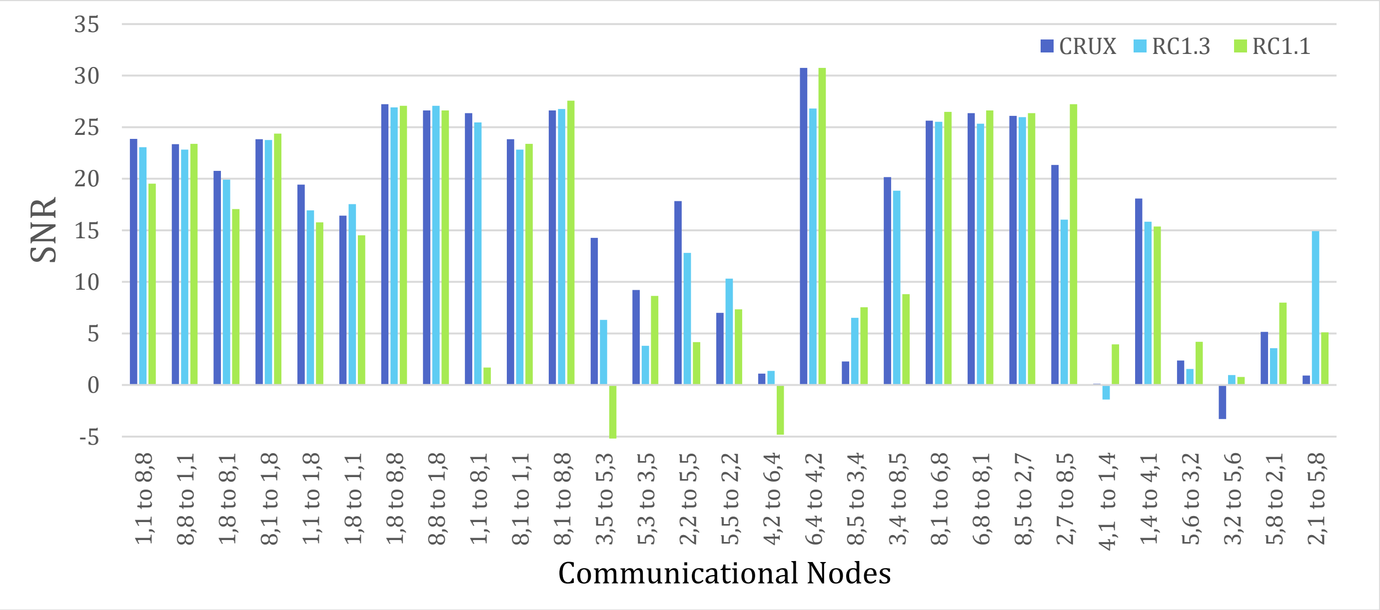

Table 22: Router comparison on the basis of SNR.

The table 10 and the graphical representation in figure 22 shows a sample of the recorded observations. The sampled observations contain a mixture of SNR results from longest links to shortest links. Followings were the observations after the simulation results.

1. The minimum and maximum SNR for CRUX is -3.30289 dB and 30.7482 dB. For *RC1.1* the minimum and maximum SNR is -6.28431 dB and 30.7482 dB while the SNR value for RC1.3 is -1.39947 dB and 27.0648 dB.
2. Negative SNR means the noise content in the signal is higher than the actual signal and the negative value of SNR has been seen for all the routers in comparison. From the figure 22 it could be seen that for a given sample set of observations, *RC1.1* has two negative values of SNR and one negative value each for *RC1.1* and CRUX. The negative values of SNR are not desirable for a proper reception of signal at the receiving end. The negative values must be minimized as much as possible by properly constructing an optical router. The SNR is reduced when the signal transverses through routers in a network because the router contains all the lossy optical elements, optical crossings and switching actively participating in production of noise and interference.
3. The average value of SNR for CRUX, *RC1.1* and *RC1.3* routers were 16.6799 dB, 14.5240 dB and 16.1444 dB. The difference of approximately 2 dB between RC1.1 and other two routers is due to the fact the crosstalk noise in the *RC1.1* router is higher compared to other routers. SNR's of *RC1.3* and CRUX are approximately similar as it could be seen from coherent crosstalk analysis that RC1.3 accounts for least crosstalk noise.
4. SNR values for *RC1.3* do not surpass the CRUX value for most of the communicational nodes because the signal power of *RC1.3* is much lower than CRUX signal power even if the crosstalk is low for *RC1.3*.
5. Even if the modelled router does not surpass the values of SNR for CRUX in all cases but the modelled router SNR values lie between 10 dB to 35 dB, which is a very promising number. It can also be seen that *RC1.3* maintains a positive SNR for cases where the CRUX SNR drops below 0 dB.

6. It can also be observed that for the longest link the SNR values for both the modelled router is above 20 dB which is a very positive outcome.
7. Based on the observations on SNR value, it can be pointed out that between *RC1.1* and *RC1.3*, *RC1.3* will stand out because it has less number of negative SNR values and the average SNR value being close to CRUX router.

6.4: Final Hypothesis.

After simulating the modelled routers on the basis of signal power, coherent crosstalk and SNR it was observed that, on basis of signal power of *RC1.1* was better than *RC1.3* while the crosstalk in *RC1.3* was significantly lower than CRUX and *RC1.1* and when it comes to SNR the average SNR for *RC1.1* is 2dB lower than CRUX and *RC1.3*. A Network-on-Chip must be power efficient and provide correct data at the receiving end. The signal power received at the destination must be higher than the crosstalk noises. At network level *RC1.1* has higher received signal power but the crosstalk noise is also higher leading to lowering of SNR which was quite evident during th router level simulation, on the contrary, *RC1.3* had signal power with lower values than both the routers in comparison but the signal power was not significantly low such that the degradation of SNR would take place. The average SNR value of *RC1.3* is comparable to CRUX and the biggest advantage of the *RC1.3* over CRUX is that the coherent crosstalk is very low, average being -36.128 dBm. From the design perspective *RC1.3* stands out among other router designs because it contains no physical waveguide crossings and no terminators. The design is symmetric with equal length distributions such that the signals must not travel longer paths. Therefore, by analysing all the facts and the figures, a hypothesis or a conclusion can be made that among the modelled routers *RC1.1* and *RC1.3*, *RC1.3* has better crosstalk noise suppression and SNR than *RC1.1* and from design perspective *RC1.3* has less crossings and the input-output links within a router is smaller with less number of optical elements.

The design of *RC1.3* is such that the physical waveguide crossing and the optical terminators are avoided which has helped in reducing crosstalk noise and losses. *RC1.3* consists of 11 switching elements for routing while CRUX uses 12 and maximum number of physical crossing in CRUX is 1 while in *RC1.3* is 0, the crosstalk noise is due to the crossing in CSE's. The footprint of both the routers is almost the same, both the router uses passive routing and uses one CSE to switch to two different outputs thereby saving on CSE. The waveguide length distributed across *RC1.3* is of equal length to maintain symmetry. *RC1.3* outperforms CRUX with respect to coherent crosstalk with average value being -36.128 dBm and -29.155 dBm respectively. From SNR point of view, average SNR value is almost equal, approximately 16 dB, which is a very reliable figure when it comes to Network-on-Chips and it has also been shown earlier that the negative SNR value for CRUX is higher than *RC1.3*. When it comes to signal power on the destination side, the values obtained for *RC1.3* are lower than the CRUX router. Although *RC1.3* from design point of view contains lower number of crossings, no terminators still the signal power loss is more because of the waveguide bendings inside the router structure. From the figure 10, it can be seen that the signal path is accompanied with waveguide bending which can lead to signal loss in terms of bending loss of 0.005 dB per bending. For example if the signal travels from west input to east output then the signal will face 4 bendings which leads to a loss of 0.02 dB, this loss will increase at network level communication. Overall, a conclusion can be provided that the *RC1.3* has the capability to replace the CRUX router because its crosstalk noise is very low and the SNR is comparable to CRUX, one area of improvement could be signal power.

The positive outcome of the *RC1.3* optical routers are:

1. Simple router design.
2. Minimum number of waveguide crossings, MRs.
3. No optical terminators used.
4. Low crosstalk noise power.
5. Acceptable SNR.
6. Smaller footprint.
7. Evenly distributed or balanced optical router.

The limitations of the RC1.3 optical routers are:

1. Signal power at receiving end is lower than CRUX.
2. Noise power at input port is higher than CRUX.
3. North-South communication inside the router requires switching action i.e. no passive path.
4. Long link length from North to Ejection port, although passive path exists.

……………

Chapter 7.

Thermal Behaviour of Modelled Router using OTEMP tool.

Optical interconnects is an emerging communication technique which has the potential to provide ultra-high bandwidth and low latency communication. The intrinsic characteristic of photonic devices i.e. thermal sensitivity proves to degrade the performance of the photonic devices. The Chip temperature fluctuates spatially across the chip `and the steady state temperature can vary significantly under typical operating conditions. As a result of thermo-optic effect, temperature variations can potentially cause power degradation. An optical interconnect thermal model is required to understand the effect of temperature on the optical system. OTEMP is used to create thermal models for both WDM-based and single wavelength based optical links in optical interconnects. OTEMP is C++ based program which is used to analyze thermal aware power consumption as well as optical power loss for optical links under temperature variations. The input to the OTEMP tool includes photonic device parameters, optical link configurations and the temperature variations. OTemp models the thermal effect in component levels and then arrives at a system-level thermal model according to the relationship between optical components in optical link.

All the inputs to the OTEMP tool are provided as text files. The parameter text file consists of the photonics parameters like the room temperature, VCSEL wavelength, and average power consumed on turning on MR etc. The configuration file hold the configurations for a WDM or Single wavelength optical link, it includes options which allows the use of on-chip or off-chip lasers, direct modulations using VCSELs or BOME (Basic Optical Modulating elements), number of active and passive switching element in an optical link etc. The output of OTEMP tool are text files which provide worst case and average case power consumption for changes in temperature. The power consumptions provided as output considers with or without thermal adjustment. As OTemp provides the option of on-chip and off-chip laser source it also includes total power consumption as well as on-chip power consumptions.

Parameter	Description	values
T_0	Room temperature in degree	25
Lambda_VCSEL_0	VCSEL wavelength at room temperature in nm	1550
Row_VCSEL	VCSEL temperature-dependent wavelength shift in nm/degree	0.09
Alpha	VCSEL minimum threshold current, in mA	2.4
Beta	A coefficient related to VCSEL threshold current	0.00075
T_th	the temperature at which the VCSEL threshold current is minimum	40
epsilon	the slope efficiency of VCSEL at 0 degree	0.403
gamma	a coefficient related to the VCSEL slope efficiency	0.00217
L_MR_resonance_peak	MR insertion loss at the resonance peak, in dB	0.5
row_MR	MR temperature-dependent wavelength shift, in nm/degree	0.06
fabrication_sigma	Gaussian distribution SD, fabrication error	0.4
P_MR_on	the average power consumed for turning on MR, in mW	0.02
Modulation_speed	the modulation speed of the VCSEL, in Gbps	10
S_RX	the receiver sensitivity, in dBm	-14.2
L_propagate	waveguide propagation loss, dB/mm	0.17
L_crossing	waveguide crossing loss, 0.12dB/crossing	0.12
link_length	length of the optical link, in mm,	20*
crossing_number	the number of waveguide crossing in the optical link	10*
E_serializer	the serializer energy consumption, in pJ/bit	0.16
E_driver	VCSEL driver energy consumption, in pJ/bit	0.1125
E_PD	the deserializer energy consumption, in pJ/bit	0.0003
E_deserializer	the deserializer energy consumption, in pJ/bit	0.128
E_TIA_LA	the TIA-LA energy consumption, in pJ/bit	0.3375
U_slope	the slope of the U(V)-I(mA) characteristic curve of the VCSEL	0.0729
U_th	the intercept of the U(V)-I(mA) characteristic curve of the VCSEL	1.0135
P_thermaltuning	power consumption of thermal-based adjustment per microresonator, in mW/nm	3.5
lambda	laser wavelength[M-1-i]=lambda-i*channel_spacing, in nm	1550
elec_switch_off_on	positive, blue-shift when turned on by electronic-based switching, in nm	0.4
thermal_switch_off_on	negative, red-shift when turned on by thermal-based switching, in nm	-0.4
modulation_0_1	positive, blue-shift of electronic-based modulation to data "1", in nm	0.4
Lambda_misplace_factor	half_3dB_bandwidth, "3" for 0.46dB drop	3
P_modulator_data_0	modulator output power for data 0	0

Table 11: Parameter List input to OTEMP Tool [3].

20*, 10* = Changes with each input output combinations

Parameter	Description	values
flag_OnChipVCSEL	"1" for using on-chip VCSEL, "0" for using off-chip VCSEL	1
flag_BOME	"1" for using BOME, "0" for using direct-modulated VCSEL	1
flag_guard_ring	"1" for using guard rings for thermal adjustment,"0" for w/o guard rings	1
flag_lambada_MR_0	"0" for using the by-default setting of MRs, "1" for using the optimal setting	0
channel_spacing	WDM channel spacing, in nm	1
M	the number of WDM wavelength	64
flag_switching	"1" for electronic-based switching, "0" for thermal-based switching	1
N_active_BOSE	the number of active BOSE stages	*1
N_park_BOSE	the number of parking BOSE stages	*3
Q	quality factor of the MRs used in the WDM-based optical link	5000

Table 12: WDM Configuration file input to OTEMP tool.

*1,*3= Changes according to input-output combinations.

The table 11 and table 12 represents the input parameter and configuration files along with values used during simulations. Before each simulation is carried out, link length and number of crossings in parameter file are updated, while in configuration file N_active_BOSE and N_park_BOSE is updated manually.

In this dissertation, the thermal effects on photonic devices of an optical link is simulated for both router level as well as for network level. In the router level simulations, for every input-output combination the link length, number of active and passive switching elements and number of crossings for each combinations in a router are recorded, each time the recorded data is passed into the OTEMP tool at the beginning of each simulation and the outputs for total power consumption both for worst case and average case for temperature range T_{min} to T_{max} is obtained. All the simulation is carried out for WDM optical link and for on-chip laser source with thermal adjust control mechanism. The simulation is carried out keeping the minimum temperature to 25°C while the maximum temperature changes from 50°C to 120°C for each simulation. For router level simulation there will be 20 observations because there are 20 links for 5x5 optical router, 4 output for each input. The network level simulation is carried out for 8x8 mesh-based network topology, here the temperature change across the network architecture is considered to follow a Gaussian distribution, i.e. the edges of the network are at room temperature and the middle section of the network is at higher temperature compared to edges. For two communicating nodes at different temperature zones of Gaussian distribution, the thermal effect is considered as follows.

1. For the communicating link between two modules, the number of routers for that particular link is counted. The routing algorithm followed will be XY routing algorithm.
2. For each router falling in a particular temperature zone, router level simulation for that particular temperature is carried out and the results are recorded.
3. After router level simulation for all the routers in the communicating link and the values are recorded for individual routers, the cumulative sum of the individual router power consumption values falling in the communicating path will be the output of the total power consumption for both worst case and average case.
4. The final result is an approximation of total power consumption because the power consumption for waveguides connecting the router in a network were not taken into account.

7.1: OTEMP Simulations and Observations.

A simulation were performed for the 20 paths with change in temperature ranging from 50°C to 100°C. The router under consider is the modelled router *RC1.3*. The following tables 13 and 14 shows simulation results for total power consumption with and without temperature adjustment for 50°C. By observing the results, a marked differences in the power consumption is seen for both with and without thermal adjustment. The power consumption for without temperature adjustment is very high in order of 10^6 mw for worst case and 10^15 mw for average case. These values are way too high and hence a control mechanism is required to reduce the power consumption. The power adjustment is done via a control system where power of the laser source is adjusted by comparing it with a reference power at a particular temperature. The changes are seen in table 14.

Path	Link_length(mm)	N_active	N_passive	# crossings	Pow Con. WC. mw	Pow Con. AC (mw)
Injection-North	0.05	3	0	0	1.51311	1.9506
Injection-East	20.15	3	4	3	2.10291	2.54889
Injection-South	14.58	2	4	3	1.96197	2.36326
Injection-West	17.06	2	3	3	1.94249	2.40206
North-Ejection	33.72	2	6	4	2.50522	2.67086
North-East	14.64	3	1	1	1.6668	2.11471
North-South	19.63	3	3	3	1.95685	2.40524
North-West	28.08	3	3	4	2.02664	2.41233
East-Ejection	23.58	3	3	4	1.98919	2.41233
East-West	19.08	2	4	4	1.9938	2.36772
East-South	16.58	3	3	4	1.94374	2.40234
East-North	11.86	3	3	3	1.91678	2.39631
South-North	9.18	2	4	3	1.93564	2.35952
South-Ejection	19.13	3	4	3	2.09525	2.54784
South-West	16.58	3	4	4	2.08224	2.54604
South-East	10.16	3	1	1	1.65374	2.10724
West-Ejection	14.59	3	1	1	1.66664	2.11462
West-North	14.82	3	4	3	2.06638	2.54383
West-South	10.16	3	2	2	1.7797	2.25005
West-East	14.78	2	4	2	1.95924	2.36288

Table 13: OTEMP Simulation Results for 50˚C with thermal Adjustment

Path	Link_length(mm)	N_active	N_passive	# crossings	Pow Con. WC mw	Pow Con. AC mw
Injection-North	0.05	3	0	0	81116.5	$2.31408x10^{11}$
Injection-East	20.15	3	4	3	$1.184x10^{6}$	$1.81486x10^{15}$
Injection-South	14.58	2	4	3	200472	$8.87449x10^{13}$
Injection-West	17.06	2	3	3	734125	$2.33316x10^{14}$
North-Ejection	33.72	2	6	4	$1.5175x10^{6}$	$1.57x10^{16}$
North-East	14.64	3	1	1	339181	$4.6571x10^{12}$
North-South	19.63	3	3	3	897558	$2.85x10^{14}$
North-West	28.08	3	3	4	$1.8369x10^{6}$	$5.8428x10^{14}$
East-Ejection	23.58	3	3	4	$1.2918x10^{6}$	$4.107x10^{14}$
East-West	19.08	2	4	4	301101	$1.333x10^{14}$
East-South	16.58	3	3	4	747218	$2.374x10^{14}$
East-North	11.86	3	3	3	488872	$1.559x10^{14}$
South-North	9.18	2	4	3	131490	$5.81491x10^{13}$
South-Ejection	19.13	3	4	3	$1.0933x10^{6}$	$1.6755x10^{15}$
South-West	16.58	3	4	4	946458	$1.45032x10^{15}$
South-East	10.16	3	1	1	238993	$3.2794x10^{12}$
West-Ejection	14.59	3	1	1	337858	$4.6389x10^{12}$
West-North	14.82	3	4	3	780455	$1.1957x10^{15}$
West-South	10.16	3	2	2	319827	2.1096610^{13}
West-East	14.78	2	4	2	192705	$8.5298x10^{13}$

Table 14: OTEMP Simulation Results for 50˚C without thermal Adjustment

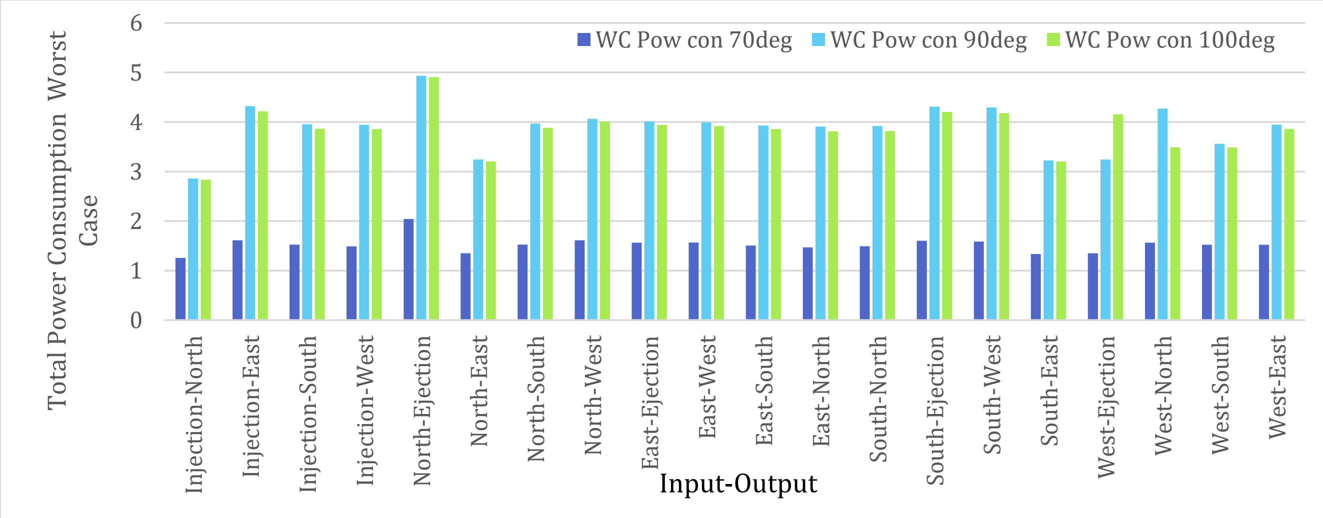

Figure 23: Worst case (WC) power consumption for changes in temperature.

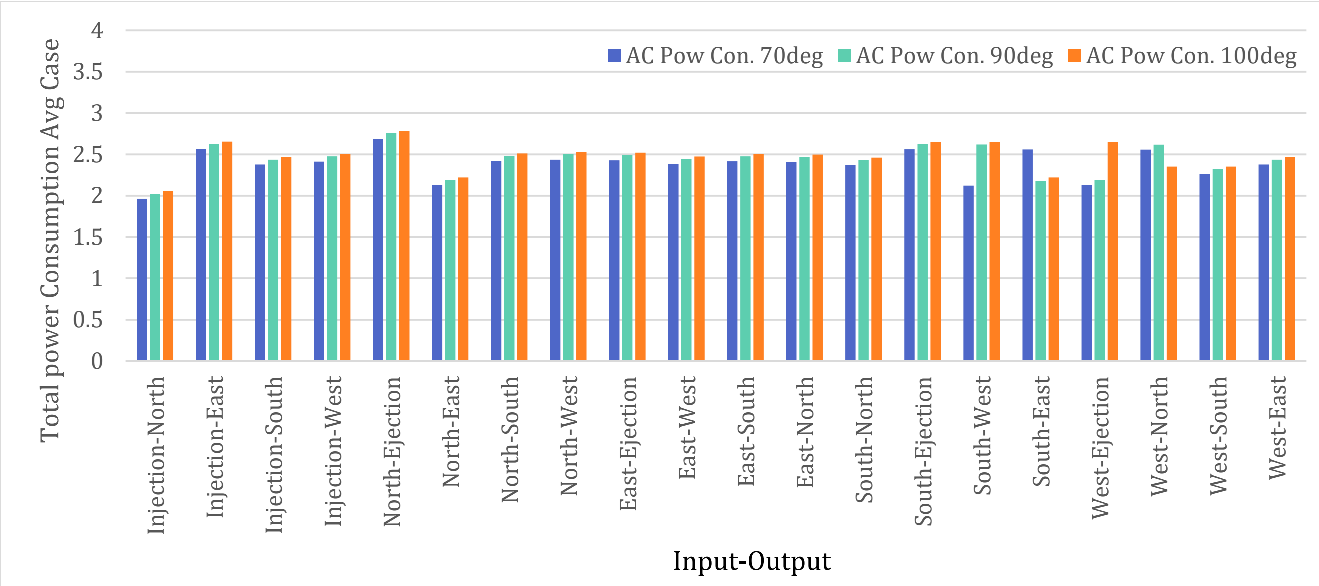

Figure 24: Average case (AC) power consumption with changes in temperature.

The above figures 23 and 24 provides simulations results with maximum temperature changing from 70˚C to 100˚C with thermal adjustment. From this simulations results some interesting observations came forward as follows.

1. For 70˚C, 90˚C and 100˚C the rise in temperature causes an increase in average case total power consumption.
2. For worst case power consumption, there is a marked increase in power consumption from 70˚C to 90˚C but the power consumptions drops when the temperature increases further by 10˚C, reason behind this observation could be due to overcompensation from the control system.

3. The power consumption without thermal adjustment is very high and the control system brings down the power consumption when thermal adjustment mechanics is implied.
4. For the same number of waveguide crossings, active and passive MRs, the power consumptions is proportional to the link length.
5. For approximately same link length and same number of crossings and active MRs, it is found that the link with more number of passive MRs possess higher values of the total power consumption.
6. An interesting observation was that the longest link without thermal adjustment (values not shown in the document) is not always the highest power consuming link. For example, for temperature 90°C ,the path North-Ejection with link length 33.72 mm has a power consumption of 1.5175x10^6 mw while for path North-West with link length 28.08 mm has the power consumption of 1.8369x10^6 mw. But, the values corresponding to thermal adjustment do not show the same observation because the thermal control system overcompensates for thermal changes.
7. For almost the same link length it was seen that the total power consumption depends on the number of active and passive switching elements and also the waveguide crossings. For example, the Injection-South path contains a total of 9 elements while the West-Ejection path contains a total of 5 elements, therefore the power consumed by path Injection-South is high.
8. For the same link length, same active and passive elements and same number of crossings, the worst case and average case power consumption for each link are the same.
9. The average case values increases as the temperature increases but for worst case values tends to decrease as it was observed from 50°C to 70°C and then increase with further with increase in temperature.
10. From simulations results it was observed that for changing temperature, the power consumption for path Injection-East is more than the power consumption for path

East- Ejection. These links have the same number of elements but the link length of the former is less than the later. This observation is unusual because according to the statistics the former path should have less power consumptions than the latter part and this behaviour remains the same for changes in temperature.

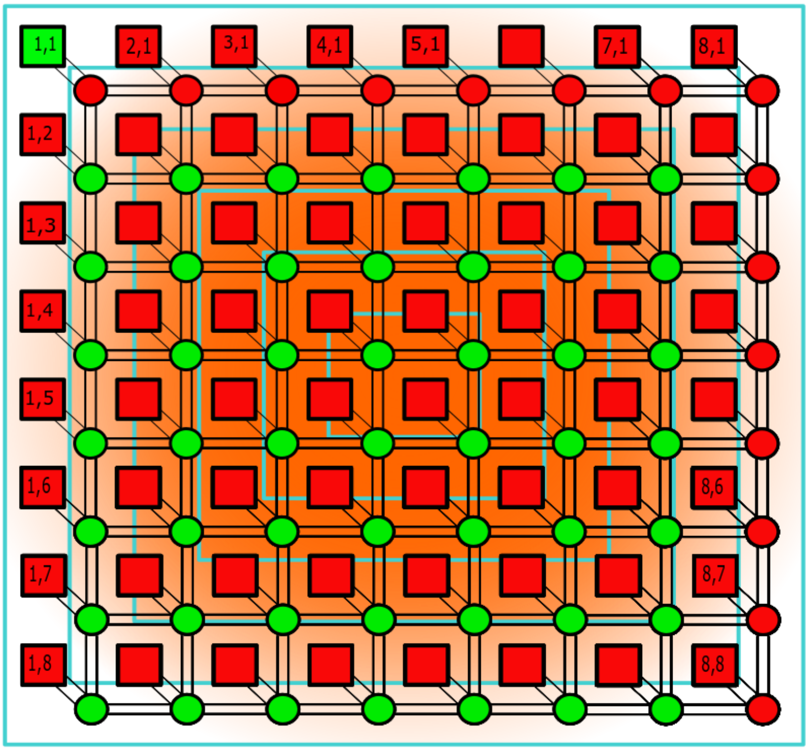

Figure 25: Gaussian distribution of temperature across the chip.

The previous observations were based on simulation carried out on OTEMP on router level. In the following section, network level OTEMP Simulation with varying temperature across the chip, the temperature is assumed to be a Gaussian distribution across the chip as shown figure 25. In the figure 25, the temperature gradient is shown where the darker shade at the centre corresponds to higher temperature and the lighter shade at the edges of the chip corresponds to lower temperature. The variation of temperature across the chip plays a vital role in deciding the total power consumption of the chip. The variation of temperature across the chip creates a variation in power consumption across the optical network because it is seen that the optical router's power consumption changes with changes in temperature. If the temperature distribution is assumed to be Gaussian distributed, which implies that the centre of the chip is assumed to be at temperature higher than the edges of the chips, therefore the routers located at the centre of the chip will consume more power than the edge routers. The Gaussian distribution of temperature across the chip creates a virtual temperature distribution over the network on-chip and helps in approximating the pattern of temperature variation, which is helpful in approximating the power consumption if a signal travels through routers in different temperature zones or hotspots. The analysis of thermo-optic effect on the network level provides data which can be analysed in optimizing networks with respect to temperature variations. The data will help in reducing the power consumption by providing information about the temperature at which the power consumption goes beyond the permitted value. The Information will allow the designers to carefully place the optical router by avoiding the high temperature hotspots on the chip.

OTEMP is a simulation tool which provides details about worst case and average case power consumptions in optical communication links for a given temperature range. Before the simulation data was provided, a table was prepared which contained columns with the communicating modules, the module's coordinates (x, y) taking part in communication, number of active and passive elements and numbers of waveguide crossings taking place in each router in the communicating link and the link length. The simulation is carried out for each router in the communication link for the particular temperature region they are situated in according to the Gaussian distribution. After all the simulations were carried out for all the routers in a communicating link , the power consumptions were added up to get an approximate power consumption for the link in the network.

Coordinates	Temperature° C	Length	Crossing	Active	Passive	Pow WC mw	Pow AC mw
1,3	35	2.5927	3	1	4	2.04259	2.14017
2,3	50	1.6736	2	0	4	1.71331	1.99631
3,3	70	1.6736	2	0	4	1.39676	2.01223
4,3	90	1.6736	2	0	4	3.26382	2.06561
5,3	90	1.6736	2	0	4	3.26382	2.06561
6,3	70	1.6736	2	0	4	1.39676	2.01223
7,3	50	1.6736	2	0	4	1.71331	1.99631
8,3	35	1.52135	5	1	1	2.01241	1.71531
1,3 - 8,3	total	14.1556	20	2	29	16.80278	16.00378

Table 15: Worst case and Average case power consumption for variation in temperature.

Coordinates	Temperature◌ ̊C	Length	Crossing	Active	Passive	Pow WC mw	Pow AC mw
1,3	75	2.5927	3	1	4	2.58969	2.20287
2,3	80	1.6736	2	0	4	1.99151	2.03591
3,3	100	1.6736	2	0	4	3.218	2.09858
4,3	110	1.6736	2	0	4	3.24847	2.14799
5,3	110	1.6736	2	0	4	3.24847	2.14799
6,3	100	1.6736	2	0	4	3.218	2.09858
7,3	80	1.6736	2	0	4	1.99151	2.03591
8,3	75	1.52135	5	1	1	1.94024	1.76361
1,3 - 8,3	total	14.1556	20	2	29	21.44589	16.53144

Table 16: Worst case and Average case power consumption for increase in temperature.

Table 15 & 16 show the worst case and average case power consumption for variation in temperature for thermally adjusted case. The table 15 shows a communication between two modules located at (1, 3) and (8, 3). The signal must be routed from source to destination via routers in an optical link. This communication link has 8 optical routers and each of the optical routers is at a different temperature region, hence each optical router will have different power consumption value. While Table 16 shows the effect on power consumption for change in temperature for the same communication link. The following were the observations.

1. It can be seen that there is a marked difference in the worst case power consumption column for the changes in temperature.
2. It was observed that for doubling the values of temperature the power consumption almost doubles.
3. The average power consumption shows a marginal rise in power consumption.
4. It was observed that a router with shorter link and at higher temperature has almost the same power consumption when compared to link with longer link and at lower temperature.

From the simulation results, the effects of temperature change in optical link can be observed and the values show the criticality of the rise in chip temperature. As we know ,the temperature varies spatially across the chip and it’s very difficult to predict the change across the chip but this type of simulation will help the designers to avoid placing interconnect networks in regions where there is a risk of change of temperature is high.

Chapter 8.

Conclusion

The primary objective was to model an optical router which could outperform the previously proposed optical router like CRUX, Cygnus, and Crossbar etc, and also simulate the effects of temperature on the modelled optical router. The secondary objective of this dissertation was to provide a survey of existing optical network on-chip and the mechanism of signal transversal across the network with the help of the optical router and the effects of temperature on the power consumptions during an optical communications across an optical network. The modelling and simulation of the router was achieved via a simulation cum modelling tool called CLAP. Approximately, 10 – 11 routers were modelled but after simulation and evaluation two routers were chosen based on the received signal power, amount of crosstalk noise and SNR. These two routers were named *RC1.1* and *RC1.3*. Out of these two modelled routers, *RC1.3*, had very simple and symmetric design with less number of waveguide crossing and MRs. *RC1.3* was compared with the CRUX optical router in terms of SNR, signal Power and crosstalk and the results were overwhelming as the crosstalk noise for *RC1.3* was very low and SNR was comparable with CRUX router but the received signal power for *RC1.3* was lower than the CRUX. From the comparison, a hypothesis elaborated the reason for choosing *RC1.3* as the best performing router between the designed routers. It also pointed out the facts which made RC1.3 better than CRUX router and also provided the limitations of RC1.3 optical router design and pointed out the future improvements which could make it more superior than existing ones. The Thermo-optic effect on the ONoCs is very critical in determining the performance of the ONoCs and hence we simulated the modelled router in OTEMP and found some interesting fact about how the number of active and passive elements, waveguide crossings and the link lengths along a communication path can have an impact on the power consumption with the changes in temperature. The simulation results of OTEMP can guide the designer in avoiding the region with higher temperature regions on-chip and hence lowering down the power consumption values. All in all, it can be concluded that ONoCs are the future interconnect and with proper designing and awareness it is possible to deploy this type of interconnect in real systems. The work has provided a novel optical router, RC1.3, which has better crosstalk noise reduction values and good SNR values to substitute the CRUX optical router but still received signal power is not at par with the CRUX router. Improving the signal power values will be a challenge for the future and designers can work on the modelled routers to make it one of the most efficient optical routers to be deployed in real systems and satisfy each and every requirement of future computing systems.

………………

References

[1]. Yaoyao Ye, Xiaowen Wu, Jiang Xu, Wei Zhang4, Mahdi Nikdast5, Xuan Wang, "*Holistic Comparison of Optical Routers for Chip Multiprocessors".*

[2]. M. Nikdast and J. Xu. Crosstalk noise and loss analysis platform (CLAP). [Online]. Available: http://www.ece.ust.hk/ eexu/index files/ crosstalk.html

[3]. Yaoyao Ye, Jiang Xu, Xiaowen Wu, Wei Zhang, Xuan Wang, Mahdi Nikdast, Zhehui Wang, Weichen Liu, "System-Level Modeling and Analysis of Thermal Effects in Optical Networks-on-Chip", IEEE Transactions on Very Large Scale Integration Systems, vol. 21, no. 2, pp. 292-305, February 2013.

[4]. *Yaoyao Ye, Zhehui Wang, Peng Yang, Jiang Xu, et al.; IEEE Transactions on Computer-Aided Design of Integrated Circuits and Systems, vol. 33, no. 11, pp. 1718-1731, November 2014*

[5]. R. Ji, L. Yang, L. Zhang, Y. Tian, J. Ding, H. Chen, Y. Lu, P. Zhou, and W. Zhu, "Microring-resonator-based four-port optical router for photonic networks-on-chip," Opt. Express 19(20), 18945–18955 (2011).

[6]. Ruiqiang Ji, Lin Yang, Lei Zhang, Yonghui Tian, Jianfeng Ding, Hongtao Chen, Yangyang Lu, Ping Zhou, and Weiwei Zhu," Five-port optical router for photonic networks on-chip" 10 October 2011 / Vol. 19, No. 21 / OPTICS EXPRESS 20258.

[7]. Lin Yang, Ruiqiang Ji, Lei Zhang, Yonghui Tian, Jianfeng Ding, Hongtao Chen, Yangyang Lu, Ping Zhou, and Weiwei Zhu, *"Optical routers for photonic networks-on-chip,"* Optoelectronic Materials and Devices VI, edited by Guang-Hua Duan, Proc. of SPIE-OSA-IEEE.Asia Communications and Photonics, SPIE Vol. 8308, 83081E · © 2011 SPIE-OSA-IEEE CCC code: 0277-786X/11/$18 · doi: 10.1117/12.902768

[8]. Huaxi Gu, Jiang Xu, "*Design of 3D Optical Network-on-Chip,"* 978-1-4244-4412-0/09/$25.00 ©2009 IEEEAuthorized licensed use limited to: Hong Kong University of Science and Technology. Downloaded on July 26, 2010 at 13:15:42 UTC from IEEE Xplore. Restrictions apply.*(PDF) Design of 3D Optical Network-on-Chip*. Available from: https://www.researchgate.net/publication/224586430_Design_of_3D_Optical_Network_on_Chip [accessed Apr 05 2020].

[9]. Yue Wang, Zheng Chen ; Ke Chen ; Kang Wang ; Huaxi Gu, "An optimized optical router for mesh based Optical Networks-on-Chip," 2015 14th International Conference on Optical Communications and Networks (ICOCN) @ Nanjing, China.

[10]. Rui Min, Ruiqiang Ji, Qiaoshan Chen, Lei Zhang, Lin Yang, “A Universal Method for Constructing N-Port Nonblocking Optical Router for Photonic Networks-On-Chip” JOURNAL OF LIGHTWAVE TECHNOLOGY, VOL. 30, NO. 23, DECEMBER 1, 2012.

[11]. Xiaowen Wu ; Jiang Xu ; Yaoyao Ye ; Xuan Wang ; Mahdi Nikdast ; Zhehui Wang ; Zhe Wang, “An Inter/Intra-Chip Optical Network for Manycore Processors” IEEE TRANSACTIONS ON VERY LARGE SCALE INTEGRATION (VLSI) SYSTEMS, VOL. 23, NO. 4, APRIL 2015.

[12]. Yaoyao Ye, Jiang Xu, Xiaowen Wu, Wei Zhang, Weichen Liu, Mahdi Nikdast, Xuan Wang, Zhehui Wang, Zhe Wang,”Thermal Analysis for 3D Optical Network-on-Chip Based on a Novel Low-Cost 6x6 Optical Router,” 978-1-4577-1619-5/12/$26.00 ©2012 IEEE.

[13]. Yaoyao Ye, Zhehui Wang, Peng Yang, Jiang Xu, Xiaowen Wu, Xuan Wang,” System-Level Modeling and Analysis of Thermal Effects in WDM-Based Optical Networks-on-Chip” 978-1-4673-5762-3/13/$31.00 ©2013 IEEE.

[14]. Yaoyao Ye, Xiaowen Wu, Jiang Xu, Mahdi Nikdast, Zhehui Wang, Xuan Wang, Zhe Wang, “System-Level Analysis of Mesh-Based Hybrid Optical-Electronic Network-on-Chip,” 2013 IEEE International Symposium on Circuits and Systems (ISCAS).

[15]. Mahdi Nikdast, “ Signal-to-noise Ratio in Optical Interconnection Networks: Analysis, Modeling, and Comparison” A Thesis Submitted to The Hong Kong University of Science and Technology in Partial Fulfilment of the Requirements for the Degree of Doctor of Philosophy in the Department of Electronic and Computer Engineering December 2013.

[16]. Yiyuan Xie, Mahdi Nikdast, Jiang Xu, Wei Zhang, Qi Li, Xiaowen Wu, Yaoyao Ye, Xuan Wang, Weichen Liu, “Crosstalk Noise and Bit Error Rate Analysis for Optical Network-on-Chip,” Design Automation Conference, Anaheim, CA, 2010, pp. 657-660.

[17]. Y. Xie et al., "Formal Worst-Case Analysis of Crosstalk Noise in Mesh-Based Optical Networks-on-Chip," in IEEE Transactions on Very Large Scale Integration (VLSI) Systems, vol. 21, no. 10, pp. 1823-1836, Oct. 2013.

[18]. On Chip Optical Waveguide Interconnect: the Problem of the In/Out Coupling. Chapter in Springer Series in Optical Sciences · May 2007.

[19]. “Silicon microring resonators “ Wim Bogaerts* , Peter De Heyn, Thomas Van Vaerenbergh, Katrien De Vos, Shankar Kumar Selvaraja, Tom Claes, Pieter Dumon, Peter Bienstman, Dries Van Thourhout, and Roel Baets. Laser Photonics Rev. **6**, No. 1, 47–73 (2012) / **DOI** 10.1002/lpor.201100017.

[20]. Sebastian Werner, Javier Navaridas, and Mikel Lujan. 2017. A Survey on Optical Network-on-Chip Architectures. *ACM Comput. Surv.* 50, 6, Article 89 (December 2017), 37 pages

[21]. Sanju V and N. Chiplunkar, "Design and implementation of mesh and torus for network on chip based system," 2015 International Conference on Trends in Automation, Communications and Computing Technology (I-TACT-15), Bangalore, 2015, pp. 1-4, doi: 10.1109/ITACT.2015.7492661.